

REPORT DOCUMENTATION PAGE			Form Approved OMB No. 0704-0188	
Public reporting burden for this collection of information is estimated to average 1 hour per response, including the time for reviewing instructions, searching existing data sources, gathering and maintaining the data needed, and completing and reviewing the collection of information. Send comments regarding this burden estimate or any other aspect of this collection of information, including suggestions for reducing this burden to Washington Headquarters Services, Directorate for Information Operations and Reports, 1215 Jefferson Davis Highway, Suite 1204, Arlington, VA 22202-4302, and to the Office of Management and Budget, Paperwork Reduction Project (0704-0188), Washington, DC 20503.				
1. AGENCY USE ONLY (Leave blank)		2. REPORT DATE 24 March 1997		3. REPORT TYPE AND DATES COVERED Conference Proceedings
4. TITLE AND SUBTITLE 10th European Drag Reduction Working Meeting			5. FUNDING NUMBERS F6170897W0088	
6. AUTHOR(S) Conference Committee				
7. PERFORMING ORGANIZATION NAME(S) AND ADDRESS(ES) Herrmann-Fottinger Institut Fuer Stroemungsmechanik Strasse Des 17. Juni 135 Berlin 10623 Germany			8. PERFORMING ORGANIZATION REPORT NUMBER N/A	
9. SPONSORING/MONITORING AGENCY NAME(S) AND ADDRESS(ES) EOARD PSC 802 BOX 14 FPO 09499-0200			10. SPONSORING/MONITORING AGENCY REPORT NUMBER CSP 97-1031	
11. SUPPLEMENTARY NOTES				
12a. DISTRIBUTION/AVAILABILITY STATEMENT Approved for public release; distribution is unlimited.			12b. DISTRIBUTION CODE A	
13. ABSTRACT (Maximum 200 words) The Final Proceedings for 10th European Drag Reduction Working Meeting, 19 March 1997 - 21 March 1997 Flow Characteristics over and around Riblets, Effects of Polymer Additives to Drag Reduction, Drag Reduction by Surfactants, Biological Aspects, Control of Transition; Turbulence and Separation, Longitudinal Vortices and Two-Phase Flows...				
14. SUBJECT TERMS EOARD, International Collaboration			15. NUMBER OF PAGES 48	
			16. PRICE CODE N/A	
17. SECURITY CLASSIFICATION OF REPORT UNCLASSIFIED	18. SECURITY CLASSIFICATION OF THIS PAGE UNCLASSIFIED	19. SECURITY CLASSIFICATION OF ABSTRACT UNCLASSIFIED	20. LIMITATION OF ABSTRACT UL	

NSN 7540-01-280-5500

Standard Form 298 (Rev. 2-89)
Prescribed by ANSI Std. Z39-18
298-102

DTIC QUALITY INSPECTED 3

10th EUROPEAN DRAG REDUCTION WORKING MEETING¹

19-21 March, Berlin

An ERCOFTAC EVENT

BOOK OF ABSTRACTS

DISTRIBUTION STATEMENT A
Approved for Public Release
Distribution Unlimited

¹We wish to thank the following for their contribution to the success of this conference:
United States Air Force European Office of Aerospace Research and Development
Deutsche Forschungsgemeinschaft (German National Science Foundation)
ERCOFTAC (European Research Community on Flow, Turbulence and Combustion).

AQF00-03-0691

SESSION 1:

RIBLETS

(Wednesday Afternoon)

Heat-transfer Characteristics of Drag-reducing Riblets

Kwing-So Choi and David Orchard

*Department of Mechanical Engineering
University of Nottingham
U.K.*

The drag reduction capabilities of riblets were extensively researched in the past two decades [1] with detailed results on the near-wall boundary layer structure over the passive device [2]. The associated heat-transfer characteristics of the micro-grooved surface were studied only by a handful of researchers [3-6], all of which, however, seem to show a large increase in heat-transfer efficiency. In order to study the structure of the thermal boundary layer over the riblet surface and understand the mechanisms responsible for this apparent breakdown of the Reynolds analogy [6], further investigations into the heat-transfer characteristics of riblets are necessary.

In the present study we tried to make an accurate evaluation of the heat-transfer characteristics of slightly-heated riblet surfaces within and just outside its drag reduction regime ($s^+ < 60$). This is a continuation of the work conducted by the author's group at the University of Nottingham. The experiments were carried out by using identically constructed smooth and riblet surfaces, minimising heat losses from them due to heat conduction and thermal radiation. Measurement of surface-temperature distribution over the test plates was also carried out to demonstrate the effectiveness of these techniques in improving the experimental accuracy.

Our results seem to indicate that the heat-conduction loss to the metal supports has the largest influence on the accuracy of heat-transfer measurement. This heat loss varies from one test plate to the other, however, depending upon the gap separating the test surface from the supports. We could significantly reduce the loss by replacing the mild-steel supports with Tufnol. A further reduction in the heat-conduction loss was obtained by an inclusion of the *heat guards* at the up- and downstream edges of the test plates. In all cases, the conduction loss through the substrate of the test plates was reduced by insulating them with a layer of polystyrene board.

The heat loss due to thermal radiation was carefully examined and compensated for using the *radiation shield* [5] which covered most of the tunnel walls. It is interesting to observe that the heat loss due to thermal radiation is greater for the large-size riblets than the small-size riblets. The amount of radiation loss from the smooth surface was nearly the same as that from the small-size riblet surface. After a careful examination of these losses from the test surfaces, we can conclude that there is an increase in heat-transfer coefficient over the riblet surfaces by up to 10% without incurring a penalty for the skin-friction drag.

References

- [1] Walsh, M.J. (1990) In *Viscous Drag Reduction in Boundary Layers*, AIAA.
- [2] Choi, K-S. (1989) *J. Fluid Mech.* **208**, 417.
- [3] Walsh, M.J. & Weinstein, L.M. (1978) *AIAA J.* **17**(7), 770.
- [4] Lindemann, A.M. (1985) *J Spacecraft.* **22**(5), 581.
- [5] Choi, K-S & Hamid, S. (1991) In *Recent Developments in Turbulence Management*, Kluwer.
- [6] Choi, K-S. (1993) *Appl. Sci. Res.* **51**, 149.

THE NATURAL CONVECTION HEAT TRANSFER PHENOMANA NEAR THE SURFACE COVERED BY RIBLETS

Harri KÄÄR, Dmitri NESHUMAJEV
Tallinn Technical University

Abstract

Natural convection experiments were conducted in water and mercury near the vertical cylindrical surface covered with riblet film (3M Corporation PVC film). The groove orientations were placed both parallel and perpendicular to the flow direction. V-grooves with depths of 75 μm were used. The experiments are performed in a range of complex $(Gr \cdot Pr^2)$ up to the $3 \cdot 10^6$ for mercury and in a range of Rayleigh numbers up to the $Ra \approx 1.6 \cdot 10^{11}$ for water.

As known, the riblets may affect to the formation of vortices in the flow and are able to drag reduction in turbulent flow up to 10% at certain Re numbers. The dependence of heat transfer on riblets orientation in natural convection is not known exactly. Also for natural convection intensity affect the properties of surface material.

Some results of measurements of temperature pulsations appeared with the turbulence in medium are shown in Fig.1. The fluctuations are recorded by fast data acquisition interface for PC and presented in Fig.1 as the temperature difference between the surface of calorimeter and liquid..

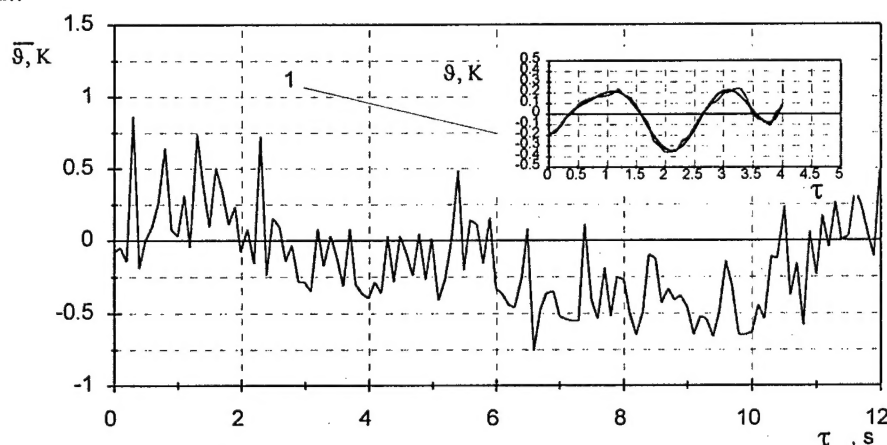


Fig. 1. The temperature difference fluctuations ($\bar{\nu} = \nu - \langle \nu \rangle$) on the riblet film surface in natural convection in mercury on time τ . Heat flux density 5887 W/m^2 ; $Gr = 2.4 \cdot 10^8$. 1- The approximation of fluctuations (fragment). θ - local surface temperature difference; $\langle \theta \rangle$ - average surface temperature difference.

The pulsation's frequency on riblets oriented towards the free convection (vertically) is two times lower of frequency for smooth surface. The spectral density of fluctuation's frequency is depend on the heat flux density. For the free convection it means that it depends on the Gr number.

Also is noticed that properties of material from which is made the calorimetric surface affect to the temperature pulsations.

IMPLEMENTATION OF DRAG REDUCTION TECHNIQUES IN NATURAL GAS PIPELINES

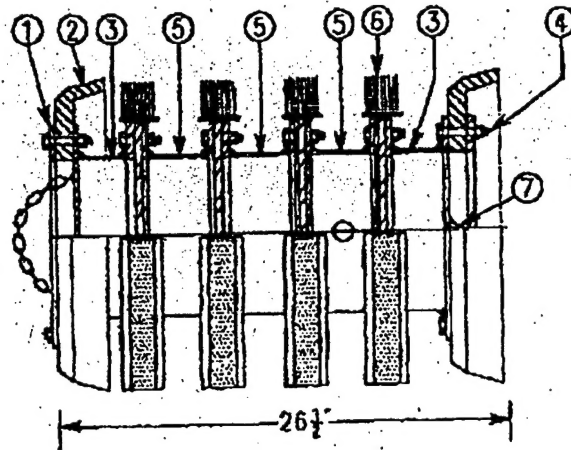
Marvin H. Weiss

NOVA Research & Technology Corporation
Calgary, Alberta, Canada

Almost since its inception over forty years ago, NOVA Gas Transmission has been pursuing techniques to improve the flow efficiency of its high pressure natural gas pipeline system. Already more than twenty years ago, the economic benefit of epoxy coating the internal surface of large diameter pipes was recognized and implemented as new pipeline was added to the system. Moreover, since the late 1980s, NOVA has been actively researching new techniques which would further increase throughput of natural gas in the existing pipe network and improve efficiency of new installations.

As a result of several research projects, a novel technique referred to as 'scribbles' has been developed. This pressure drop reduction method involves very small grooves—about the width of a human hair—which are scratched into the internal pipe surface in the direction of flow. The mechanism of the grooves is very similar to that of riblets, only that the geometrical dimensions and shape are not as precise nor as regular. Careful laboratory tests on small diameter steel pipes (\varnothing 100 mm) indicated at least 5% less pressure drop in grooved pipe when compared to the same pipe in its as-manufactured state. The grooves were scribed into the pipe wall by pulling small pigging tools, with flat wire steel brushes, through the pipe.

In the past year, a full scale field trial was completed in which a flat wire brush pig, as shown in the attached figure, was sent through an 11.6 km section of 400 mm diameter pipe which was in operation. Flow measurements at high Reynolds number ($\sim 3 \times 10^6$) before and after the pigging run indicated a 10% reduction in pressure drop, likely due to the combined effect of cleaning the internal surface and the formation of scribbles. Further field tests are planned for the coming year after which plans for further implementation in NOVA's almost 22,000 km of high pressure natural gas pipe will be developed.



Flat wire brush pfg used in field trial.

Computation of three-dimensional Stokes flow over complicated surfaces (3d riblets) using a boundary-independent grid and local corrections

P. Luchini

Dipartimento di Ingegneria Aerospaziale - Politecnico di Milano
Via Golgi 40 - 20133 Milano - Italy

and

A. Pozzi

Dipartimento di Progettazione Aeronautica - Università di Napoli
P.le Tecchio - 80125 Napoli - Italy

The research of new possibilities for improving the drag-reduction characteristics of riblet surfaces induced Bechert's group in Berlin, a couple of years ago, to experiment with 3d riblet geometries, in which the riblets are periodically interrupted in an alternating pattern. The rationale was that cutting the riblets might decrease the nonlinear sloshing and allow the linear viscous drag reduction mechanism to persist up to larger riblet sizes. As soon as we were informed of these experiments, we started an effort to extend the numerical calculation of viscous protrusion heights to 3d geometries. The preliminary results of this effort, which we presented at the last EDRM in Ravello, gave the qualitative indication that an improvement (although probably a modest one) could be hoped for by changing slightly the fill-to-empty ratio of the riblets used in the experiment. However, our 3d Stokes-flow program was not at the time capable to operate with the exact geometry used in the experiments, but only with a qualitatively similar one.

The subsequent trimming and perfecting of our computation led to a general and quite unconventional numerical method for studying 3d viscous flow over complicated surfaces which can be applied to a much wider range of problems. (In particular, since this is not a boundary-integral but a volume finite-differences method, extensions to the full Navier-Stokes problem are possible.)

Several decisions were involved in the set-up of our method. First, we renounced to the boundary-integral formulation that we had adopted for 2d riblets, because in three dimensions the (iterative or otherwise) inversion of a full matrix of size $n^2 \times n^2$ (if n is the typical number of discretization points in each direction) leads to a much larger computational work than the iterative inversion of the very sparse $n^3 \times n^3$ matrix resulting from a finite-difference formulation. Second, whereas numerical calculations of flow over 2d riblet geometries have in the past been conducted by others on orthogonal curvilinear boundary-fitted grids, the complications arising from the use of a boundary-fitted grid in three dimensions (where it cannot in general be made orthogonal) induced us to opt for a boundary-independent square grid. Much of our development effort was therefore devoted to suitably interpolated boundary conditions. Third, based on our previous experience with the multigrid method (P. Luchini, *J. Comp. Phys.* **92**, 349, 1991; P. Luchini, *Int. J. Num. Meth. Fluids* **12**, 491, 1991; P. Luchini & A. D'Alascio, *Int. J. Num. Meth. Fluids* **18**, 489, 1994), we decided to adapt this, very fast, solution method to the Stokes problem. Last, in order to circumvent the difficulties classically associated with the discretization of pressure and velocities on co-located grid points we opted for the magnetization formulation (Luchini, *AIAA J.* **29**, 474, 1991) in which velocity and pressure are replaced by a new vector (which bears some mathematical resemblance to the magnetization field of magnetostatics) and a new scalar (a potential).

We shall, in this meeting, present our method, taking 3d riblets as an example. We shall also give results containing the longitudinal and transverse protrusion heights for several 3d riblet profiles, including the precise geometry used in Bechert's experiments (which he kindly disclosed to us in advance).

MEASUREMENT OF FLOW STRUCTURES IN A TURBULENT BOUNDARY LAYER OVER SMOOTH AND RIBLET SURFACES

J.G.TH. VAN DER HOEVEN

Humboldt University Berlin, University Hospital Rudolf Virchow, Lab. for Biofluidmechanics
Spandauer Damm 130, 10559 Berlin, Germany

J. WESTERWEEL and F.T.M. NIEUWSTADT

Delft University of Technology, Laboratory for Aero and Hydrodynamics
Rotterdamseweg 145, 2628 AL Delft, The Netherlands

It is conjectured that riblet surfaces effect a drag reduction by organizing the structure of a turbulent flow in the near-wall region of a turbulent boundary layer. However, direct experimental observation is inconclusive, as these are based on single-point measurement probes (like LDV) or qualitative observations with conventional flow visualization. Digital particle image velocimetry (DPIV) is a measurement technique that yields quantitative information of the instantaneous velocity field in a planar cross-section of the flow, and it is especially useful for the investigation of flow structures. We therefore decided to use this technique to make a quantitative investigation of the flow structures in a boundary layer over smooth and riblet surfaces.

The measurements were carried out in a boundary layer over a flat plate in a free-surface water flow facility. The Reynolds number was about 800 (based on the free-stream velocity and the momentum thickness). One smooth and two v-shaped riblet surfaces were investigated. The dimension of the riblets was chosen in order to compare the flow over a drag reducing ($s^+ = 17$), a smooth and a drag increasing ($s^+ = 27$) surface. In a previous investigation [1] it was demonstrated that DPIV can provide accurate measurements of the velocity in a turbulent pipe flow. We used an image acquisition system that can record high-resolution images (1000×1016 pixels) at a rate of 10 images per second, with a real-time storage capacity of 262 images.

In this experiment we focus on the so-called low-speed streaks, so we choose our measurement planes parallel to the wall, with a view area of approximately $350 \times 350 l^+$. This configuration yields the streamwise and spanwise velocity components with a spatial resolution of $5 l^+$ (i.e., 3782 velocity measurements per image), and with an accuracy of about 1% of the mean streamwise velocity. In order to obtain accurate measurements of the flow statistics we also carried out measurements with LDV; this also allows us to validate the DPIV results.

Several time series have been recorded over the three surfaces at various distances from the surface, ranging from the buffer layer to the outer edge of the boundary layer. The results obtained from the measurements of the flow over a smooth surface show that the velocity statistics are homogeneous within each measurement plane. To determine the turbulent flow statistics from the DPIV measurements we ensemble averaged the data over all frames of each time series. The vector maps of the instantaneous velocity relative to the mean streamwise velocity in the measurement plane ($U(y)$) show different patterns depending on the distance from the surface. Clearly, as we approach the wall the structure of the instantaneous flow changes from small structures in the outer region of the boundary layer, to elongated patterns close to the buffer layer. A preliminary qualitative comparison of the evolution of the vector maps of the series recorded at $y^+ = 13$ shows some interesting differences for the different flow cases.

From the results we can already conclude that the results for the mean velocity profile obtained with DPIV agree with those obtained with LDV. The vector maps show how the structure of the flow depends on the distance from the wall as well as on the kind of surface. We are currently investigating the series recorded close to the surface; the results will be included in the final presentation.

[1] Westerweel, J., Draad, A.A., van der Hoeven, J.G.Th. and van Oord, J. (1996) Measurement of fully-developed turbulent pipe flow with digital particle image velocimetry, *Exp. Fluids*, Vol. no. 20, pp.165-177

Effect of Riblets on Flow-Structures at Laminar-Turbulent Transition and Simulation of their Influence on Turbulent Boundary Layer

V.V. Kozlov

Institute Theoretical and Applied Mechanics
630090, Novosibirsk, Russia

In the first part of the lecture the comparison of riblet influence on turbulent boundary layer (laminar sublayer) and some structures at laminar-turbulent transition is carried out.

Then, the results of an experimental study on the influence of riblets on various structures of the laminar-turbulent transition in the Blasius boundary layer in subsonic flow such as two-dimensional Tollmien-Schlichting waves and longitudinal vortex structures of the Gortler-like or cross flow-like vortices, A-vortices and vortices excited in the wake behind a roughness [1-4] is presented. It is shown that triangular riblet profiles mounted in the direction of the flow result in an unfavorable influence on the development of two-dimensional Tollmien-Schlichting waves. On the other hand, riblets were also found to significantly affect the development of non-linear wave packets (A-vortices) giving a slower growth of their intensity and delaying their transformation into the turbulent spots. The present effect of riblets on the development of a crossflow-like single vortex and Gortler-like vortices lead up to reduction of their intensity, resulting in slow damping of the secondary traveling waves and the flow remains laminar throughout the studied region. The present riblets inhibit the transition to turbulence in the wake behind a roughness.

The possibility to use "active riblets" is discussed.

1. G.R. Grek, V.V. Kozlov, S.V. Titarenko & B.G.B. Klingmann, The influence of riblets on a boundary layer with embedded streamwise vortices. *Phys. Fluids*, 1995, 7 (10), 2504-2506.
2. G.R. Grek, V.V. Kozlov, S.V. Titarenko, An experimental study of the influence of riblets on transition, 1996, *J. Fluid Mech.*, 315, 31-49.
3. G.R. Grek, V.V. Kozlov, S.V. Titarenko, Effects of riblets on vortex development in the wake behind a single roughness element in the laminar boundary layer on a flat plate, *La Recherche Aerospatiale*, 1996 (1), 1-9.
4. A.V. Boiko, V.V. Kozlov, V.V. Syzrantsev & V.A. Scherbakov, Experimental study of secondary instability and breakdown in a swept wing boundary layer. *Proc. in IUTAM Symposium on Laminar-Turbulent Transition*, Sendai, Japan, Berlin: Springer Verlag, 1995, pp. 1-7.

SESSION 2:

POLYMER ADDITIVES

(Thursday Morning)

A critical discussion of the so-called 'momentum deficit' of drag reducing flows.

by A. Gyr¹ and A. Tsinober²

¹Inst. of Hydromechanics and Water Resources Management, ETHZ, CH-8093 Zurich

²Dept. of Fluid Mech. and Heat Trans. Eng., Tel-Aviv University, IL-69978 Tel-Aviv

Turbulent flows of drag reducing fluids (even super-diluted) exhibit the so-called "momentum deficit". This deficit is manifested in that the total stress is larger than (i.e. not balanced by) the sum of the Reynolds stress and the mean viscous stress, the latter calculated assuming the fluid possessing its Newtonian viscosity. Since there is no reason whatsoever to doubt the momentum balance the "momentum deficit" cannot be considered as real deficit and is a clear indication that drag reducing fluids are essentially Non-Newtonian in turbulent flow state, though in many laminar flows they behave almost as Newtonian.

Two sets of data acquired in flows with polymer (100 ppm Pr2360) and surfactant (1.9 mMol/l C₁₄TASal at 20 °C) additives at maximum drag reduction were used to investigate this 'momentum deficit' in more detail. It could be proved that the effect is not the result of an enhanced secondary flow as could be thought by examining the deficit function $G(y^+)$ given by:

$$G(y^+) = \left(1 - \frac{y}{R}\right) - \frac{dU^+}{dy^+} + \frac{\overline{u'v'}}{u_\tau^2} \quad \text{with} \quad \overline{u'v'} < 0$$

with y the wall distance and R the one of the axis of the pipe and $u_\tau = (\tau_w / \rho)^{1/2}$ the wall shear velocity.

The two drag reducing solutions appear to behave differently. This can be seen from a representation of the deficit in form of an effective viscosity as defined by Giesekus (1981) as

$$-\frac{\overline{u'v'}}{u_\tau^2} = 1 - \frac{y}{R} - \frac{\nu_{eff}}{\nu_0} \frac{dU^+}{dy^+}$$

For the surfactant solution one can interpret the effective viscosity in the near wall region as an increased shear viscosity. In the outer flow region a new effect must be present which would need a 20 time higher shear viscosity to be represented in a Newtonian form. For polymers the effect is not so drastic and shows a smooth behaviour. For both additives the effective viscosity has its maximum at about a wall distance of 150 viscous units.

The turbulent effective viscosity has more or less bimodal distribution as function of the wall distance, and it is seen from fig. 1 that the "effective" viscosity is in both fluids qualitatively (i.e. strongly varies across the flow cross section) and quantitatively different from the value (i.e. regular Newtonian viscosity) it should have to assume if the fluid would be Newtonian. In

other words this means that strong Non-Newtonian effects are present and no simple constitutive relation exist.

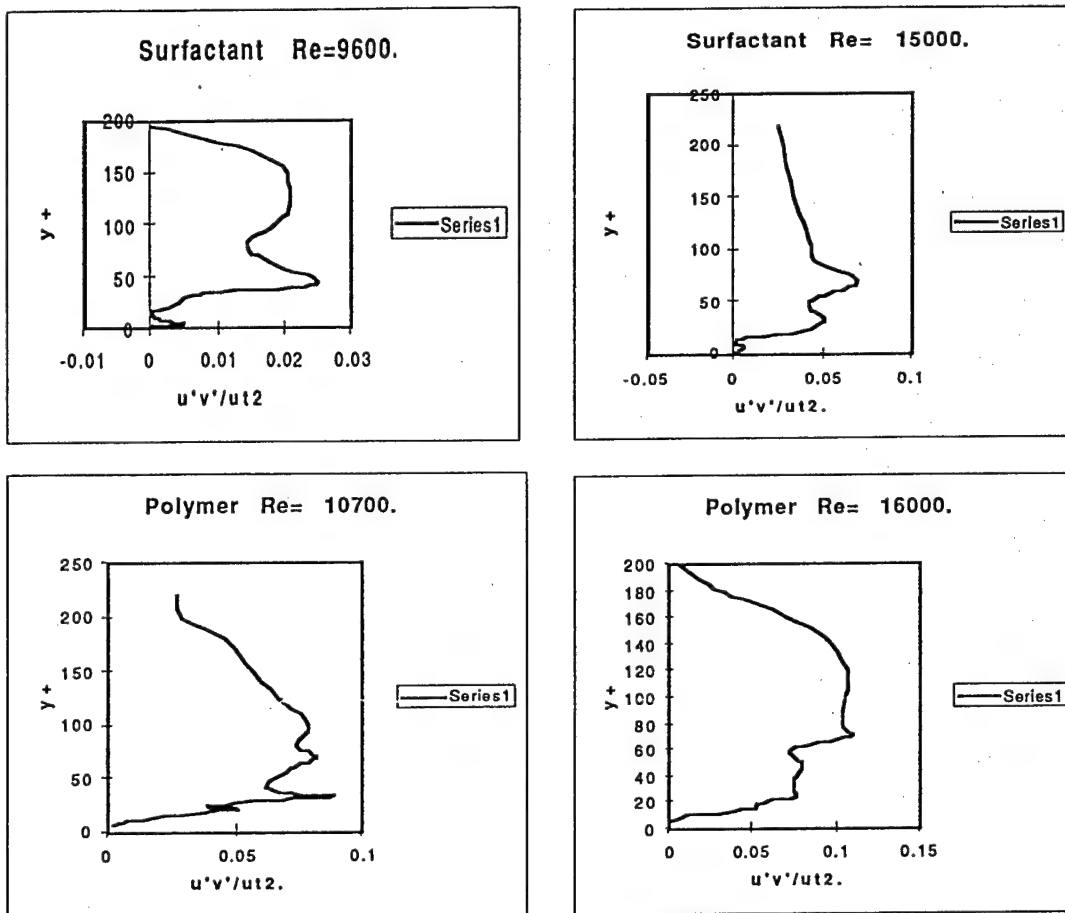


Figure 1: The momentum transport by turbulent fluctuations for the two drag reducing solutions at two Reynolds numbers. (The surfactant data from Beiersdorfer (1993), the polymer solution data from Yong (1988))

References:

- Beiersdorfer, H. 1993 Untersuchungen der Turbulenzstruktur bei maximaler Widerstandsverminderung in einer Kanalströmung einer viskoelastischen Tensidlösung. Diploma Thesis Unive. of Dortmund.
- Giesekus, H. 1981 Structure of turbulence in drag reducing fluids. Lecture Series 1981-86. Von Kármán Inst. for Fluid Dynamics. Rhode-Saint-Genèse (Belgium).
- Yong, C.K. 1988 Zur Wirkung von Polymer-Additiven auf die kohärente Struktur turbulenter Kanalströmungen. Ph. D. Thesis Univ. of Essen.

Torsten Becker [†], Bruno Eckhardt [‡]

[†] Fachbereich Physik und Institut für Chemie und Biologie des Meeres,
Carl-von-Ossietzky Universität, Postfach 25 03, D-26111 Oldenburg,
Germany
Email: t.becker@kocy.icbm.uni-oldenburg.de

[‡] Fachbereich Physik der Philipps-Universität, Renthof 6, D-35032 Mar-
burg, Germany
Email: bruno.eckhardt@physik.uni-marburg.de

Drag reduction in a turbulent shear flow based on the reduced wave vector set approximation

We employ the reduced wave vector set approximation (J. Eggers, S. Grossmann, Phys. Fluids A 3, 1958 (1991)) to build a turbulence model which imitates a plane Couette flow. The model allows for numerical integration of different constitutive relations: We focus on a corotational Maxwell fluid and a special case of the transversely isotropic fluid (J. L. Ericksen, Kolloid-Zeitschrift 173, 117 (1960)). Due to the sparing use of computer resources the model permits relaxation into the statistically stationary state of the flow and measurement of statistical averages as the flow rate and the energy dissipation within a reasonable amount of computing time. We present results identifying the anisotropic fluid as a drag reducer. The Maxwell fluid on the other hand dissipates more energy than the usual Newtonian fluid at the same flow rate. In addition to gross flow properties we show results concerning the turbulence statistics.

INFLUENCE OF MOLECULAR MASS OF PEO ON VIRK ULTIMATE DRAG REDUCTION

KULIK V.M.

Institute of Thermophysics, Siberian Branch of Russian Academy of Sciences. Novosibirsk,
630090, Russia

The experimental results of investigation of drag reduction change along the tube for PEO-solutions with different molecular mass are presented. The presence of drag reduction growth, maximum of drag reduction and degradation slope is shown. The method of calculation of hydrodynamic friction based on measuring of pressure drop is analyzed. It is shown, that contribution to pressure drop from kinetic energy of flow can be considerable. The method of correction is based on calculation of kinetic energy coefficient for Bernoulli equation is suggested.

The maximum drag reduction does not depend on molecular mass of PEO in studied region (0.8-3.25 mln) and is close to ultimate value. The increase of molecular mass shifts the place of maximum drag reduction appearance to the end of tube.

He obtained results widen the range of application of Virk ultimate drag reduction law.

The Boundary Layer With Slot Injection of Polymer Solutions

**W.B. Amfilokhiev, B.A. Barbanel
N.P. Mazaeva**

The drag reduction with the help of dilute polymer solutions can be organized by injection of concentrated solution through the transversal slots. The method for the characteristics was worked out with taking into account a few factors: the influence of body size and body velocity, the quantity of injected polymer, the position of slots and their numbers. The nondimensional characteristics are found as a function of the Reynolds number and the calculation of boundary layer rate of polymer expenditure.

Similarity Criteria for the Dilute Polymer Solutions Turbulent Flows and Generalized Formulae of Friction Factors

L.S. Artjushokov, W.B. Amfilokhiev

An attempt to solve the problem of the drag reduction scale-up for dilute polymer solutions is undertaken. It is based on the theory of similarity for the non-Newtonian liquid and as a result the generalized formula for the friction factors are obtained. The main criterion of similarity in these formulae is the visco-elastic Reynolds number that includes the combination of usual Reynolds number and Deborah number. The formulae are proved with many experimental results.

The effect of polymer additives and SAS (surfactant substances) on the hydrodynamic resistance of liquid flows.

**Prof. A. B. Stupin
(Donetsk State University, Ukraine)**

1. This paper deals with the semiempirical theory of drag reduction of liquids by polymer additives in view of a structural approach. The theory is based on the mechanism of a resonant absorption of a turbulent energy by the macromolecules of polymers, the main point of which is that in a turbulent flow a polymeric molecule will be effected by spectre of turbulent perturbations, which, in accordance with the spectral theory of turbulence, can be represented as the superposition of periodical flat waves. In case of overlapping the spectre of its own frequencies of macromolecules by the frequencies of external turbulent perturbations there takes place resonant absorption of a turbulent energy, which results in the decrease of pulsation motion intensity. Taking into account orientation influence of the average motion the macromolecules of polymers will exert its main influence on the transversal pulsations of velocity, which, in its turn, results on emerging anisotrope viscosity.

In view of the conception of anisotrope viscosity we have constructed non-layer, two-and-three-layer models, which enabled us to calculate the velocity profiles and hydrodynamic resistance coefficient in turbulent flows of polymer solutions, including the maximum drag reduction.

2. We have analysed the results of practical use of polymer additives and SAS in fire-extinguishing, for impulse hydrodestruction and continuous hydrocutting of various hard materials (rocks, coal, metals, plastics, etc.). For this purpose on the basis of hydrodynamically action polymer-polyethylenoxide (PEO) we have elaborated hard water dissoluble polymeric compositions (briquettes), which have an increased mass output and make it possible to get hydrodynamically active solutions at short intervals of time. The results of natural tests of the elaborated briquettes showed that the efficiency of work of fire-extinguishing systems, hydrocutting processes and hydrodestruction of hard materials increases greatly.

THE PROMISING STUDY OF WATER-SOLUBLE COATINGS FOR DRAG REDUCTION

B.N. SEMENOV

Institute of Thermophysics, Siberian Branch of Russian Academy of Sciences. Novosibirsk,
630090, Russia

The water-soluble polymeric coatings are tempting as passive means for drag reduction since they don't need additive volumes and energy expenses for their use.

The following factors of the coating action on near-wall flows were considered in described investigations:

- a compliance of coatings on account of their water-swollen state;
- an injection of drag-reducing polymeric additives into flow;
- a variable viscosity of fluid in boundary layer near the covered wall;
- a roughness of the coating surface.

Here the duration of continuous observations of washing out of coating and its action on hydrodynamic friction, total drag and wall-pressure fluctuations was well over the duration in works of other authors (at least, by two orders): the duration of drag reduction achieved 30 minutes.

The used water-soluble compositions contain the high-molecular PEO and other components, secure for environment too.

Experiments were carried out in the running fresh water (a part of water tunnel wall was covered with water-soluble coating) and in the saline lake Issyk-Kool (2.1 m-long streamline body of revolution was towed by the tow boat). Different variations of the coating place on flowed surface were studied.

- The coating is placed in a region of turbulent boundary layer on a flat plate or a surface of cylindrical part of the streamline body with zero hydrodynamic pressure. Here an action of compliance is changed with time of washing out because of a change of thickness and viscoelastic properties of swollen layer. For a careful preparation of coating and its sufficient adhesion its surface roughness increases a little in process of washing out. The high viscosity of polymeric solution near a water-soluble coating can lead to friction increase for covered part. Drag reduction is observed downstream behind the covered part. Its depends on the dissolved PEO mass proportional to the friction on the covered surface and to its area. The time of washing out is proportional to the thickness of dry coating.

- The coating is placed in a region of positive hydrodynamic pressure and of adverse pressure gradient. Here all remarks are just the same, but the even washing out is observed for higher velocities.

- The coating is placed in a region of negative hydrodynamic pressure. Here the lump separation of water-swollen layer is possible already for small velocities. It leads to useless expenditure of polymeric coating and to strong increase of the surface roughness and accordingly to increase of friction of covered part.

- The coating is placed on the model nosing in a region of positive hydrodynamic pressure and of strong favorable pressure gradient. The laminar flow in this region is conditioned by pressure gradient. The washing out of water-soluble coating doesn't change the laminar friction on covered surface but decreases the turbulent friction downstream on the rest of model surface. Here the even washing out was observed for all considered velocities (till 18 m/s). The specific effectiveness of drag reduction (i.e. the ratio of drag reduction to dimensionless consumption of PEO) for this variant is well over one for the best variant of slot injection of PEO solutions (at least, five times). So this variant is promising for technical elaboration of drag reduction by polymer additives.

POLYMERS SUBMISSION OPTIMIZATION WITH THE HELP OF SWORD-SHAPED TIPS

V.V. Babenko

Institute of Hydromechanics
National Academy of Sciences of Ukraine, Kiev

Way of a turbulent boundary layer control with the help of the high-molecular polymeric (PEO) additives of small concentration giving unnewtonian properties to liquids, are an effective way of influence on hydrodynamic processes in a boundary layer. Such additives, in particular, reduce a level of turbulence and increase thickness of laminar sublayer resulted in significant reduction of friction resistance of a streamline surface. The effect of resistance reduction is displayed when the polymeric additives are present at a buffer zone between viscous sublayer and turbulent nucleus. There is not found out the mains question: which mechanism of polymers molecules influence on the characteristics of a boundary layer and on the physical mechanism of friction reduction. The question of coherent vortical structures development in a turbulent boundary layer of polymers water solutions is completely not investigated.

For realization of measurements of polymers water solutions submission influence on a boundary layer characteristics a model of rotation body was developed. The scheme of a model made from a plexiglas exposed. The model consists of a tail part to which cowl in form of symmetric profile is pasted. With the help of two screws, models fastens to a knife. A tail cowl is screwed behind a tail part, and a cylindrical part diameters 0.04 m and consisting from two sections is screwed in front of model. One or both sections can be installed. At installation of two sections, length of a model makes 0.415 m. In front of cylindrical section a nasal part of model, having ahead one axial and eight inclined apertures on periphery is screwed. Conic and nasal cowls is screwed on a forward axis of a nasal part so, that one or two slots of various width is possible to fix. By a nasal cowl was made in the various form and also, as well as the tail cowl, was made from a plexiglas, or from metal (brass). A model in a water tunnel and various nasal cowls exposed.

The method of conducting experiments with injection of aqueous solutions of polymers, using different amounts and concentrations, for injection through adjustable nose slits exposed in part II. Similarly, injections of other types of fluids were made through the nose slits with attachment to the model of an ogive-shaped (OT), short (SXT) and elongated (LXT) xiphoid-shaped tips. Without injection of PEO solution, the coefficient of model resistance C_x with a sword-shaped tip increased, as compared to OT, although there was insignificant increase in size of wet surface.

The results of experiments on a model with OT revealed that injection of freshly prepared polymer solution with concentration $C=0.1\%$ (curve 9) had the greatest effect on lowering resistance. Experiments on a model with SXT and LXT revealed that injection of the polymer was the most effective with SXT at $C=0.15\%$, and with LXT at $Re < 10^6$ with $C=0.1\%$, and with $Re > 10^6$ with $C=0.05\%$.

Efficiency of drag reduction by surfactants and its limitations for district heating networks

Jaroslav POLLERT

Czech Technical University in Prague

Czech republic

District heating world-wide gains in significance in regard to supply the space heating demand. It is able to promote a primary energy saving, environmentally acceptable and low-priced energy supply. Special advantages of district heating are waste heat utilisation and energy supply by combined heat and power plants. High investment costs of the heat transport and distribution network with relative small annual utilisation times are disadvantages of district heating. Thus all efforts to improve the economy of heat supply is of importance. One of the promising possibilities is using drag reducing additives in district heating systems.

Measurements were made using quarternary ammonium salts with their trade names: Habon G (Hoechst GmbH - FRG), Ethoquad T/13 (Akzo Chemicals - USA). Except of Habon G surfactant solutions were prepared by adding sodium salycilate solutions to thoroughly mixed quarternary ammonium salt dispersions or direct dissolving of salt in water.

Because of the sensitivity of surfactant additives to wall shear stress, the level of drag reduction was strongly dependent on tube diameter. As a result, the level of drag reduction at high Reynolds numbers is larger for large tubes which have not exceeded the critical wall shear stress. In polymer solutions, drag reduction is generally greater in small tubes.

Limitation of drag reduction by surfactant appears also in heating networks. For this experiments in simple network of 4 and 10 mm tubes in parallel were carried out. In network flows through small and large tubes in which the diameter ratios exceeded 2.5 : 1, drag reduction effectiveness in the small tube is surprisingly extended to higher Reynolds numbers compared with flows through a single small tube of the same diameter.

Overall heat transfer reduction in a plate fin heat exchanger was below 30 % for concentrated surfactant solution with smaller reductions when concentration was reduced. This corresponds to about 50 % reduction in the heat transfer coefficient of the surfactant solution. The average wall shear stress in the plate heat exchanger calculated from pressure drop measurements varied from 0 to 20 Pa for all tested solutions. In contradiction no significant effect of the presence of the surfactant drag reducing additive on overall heat transfer coefficient was observed in district heating field test.

Acknowledgements

This research was conducted as a collaborative project by the Department of Hydraulics and Hydrology, CTU Prague, as a part of research project Czech Grant Agency No.: 113/94/1186.

DRAG REDUCTION BY SURFACTANTS AND THE RELEVANCE OF THEIR RHEOLOGICAL PROPERTIES

Jiri Myska, Petr Stern, Jana Mutlova
Institute of Hydrodynamics AS CR, Praha, Czech Republic

Drag reducing cationactive surfactants are promising additives for district heating and cooling systems. Their capability in energy saving was shown in large scale field tests in primary heating circuits with 450 and 200mm pipes in Germany [1,2], with 200mm pipe in Denmark [3], in hydronic heating system of a building (12m³ water volume) in the USA [4], in secondary heating system of a city district with 330 apartments (40m³ water volume) in the Czech Republic [5]. Further tests with cooling water in mines with 100 to 300mm pipes were done in Ukraine [6] and also in the cooling system of a building (34 rooms) in the USA [7]. Most often used surfactants were Dobon and Habon G of Hoechst AG [1,2,3,5], Ditalan OTS or Methaupon [6], Ethoquad T/13-50 [7] and Arquad 16-50 [4] (with sodium salicylate) of AKZO Chemie.

The ability of drag reduction is often explained in connection with their rheological properties. However, it has been recently suggested that first normal stress differences [8] as well as modulus data [9] do not play any important role in drag reduction by surfactants. Thus drag reduction is probably not related to elasticity of the surfactant but rather to its viscous properties. Therefore the dynamic viscosity and elongational viscosity are characteristics considered to be relevant for drag reduction. In fact, viscosity behavior reveals remarkable characteristic property of the micelle network structure, the Shear Induced Structure.

Typical feature of a surfactant is a sudden jump of the order in magnitude from a small viscosity value to a very high one at very low shear rates, usually of the order of units of s⁻¹. It is explained by means of building a micelle superstructure. Viscosity then decreases with increasing shear rate to a minimum within a few hundred of reciprocal seconds. Further pattern of viscosity curves from the minimum shows a great variety. It can increase again like e.g. in the solution of Ethoquad T/13-50 with sodium salicylate revealing the development of a new secondary structure, or stay constant, Newtonian, like in the case of e.g. Habon G.

Absolute value of the viscosity is not only temperature and concentration dependent, but it depends on the geometry of the rheometer, too. Also shearing history is of great importance and different results are obtained by preshearing under laminar or turbulent conditions. Rheological properties of surfactants in distilled water are usually investigated in laboratories, but tap water or partly treated (decarbonated) water is used in heating and cooling systems. Some cations and anions present in water make a substantial influence on the viscosity and the shape of viscosity curves of diluted surfactants. This research is under way. We have found that temperature subdues the characteristic feature of SIS, the sudden viscosity increase at small shear rates and the attainment of high viscosity values, and that some ions cause a complete loss of SIS even at room temperature. Both cations and anions in water may decrease apparent viscosity of drag reducing surfactants, and they can even change the pattern of the viscosity curve which gives evidence of their strong impact on the micelle structure. However, drag reduction ability is lost neither with increasing temperature nor with small amounts of these ions.

Literature

- [1] Althaus W. Dissertation, Universität Dortmund, 1991.
- [2] Kleuker H.H., Althaus W., Steiff P., Weinspach P.M. Private communication.
- [3] Hammer F. Fernwärme International-FWI, Jg 22, 4, 1993.
- [4] Rose G.D., Foster K.L., Slocum V.L., Lenhart J.G. 3rd Int.Conf. on Drag Reduction, 2-5 July, University of Bristol, Bristol 1984.
- [5] Kratochvíl P., Havelka J. Report No. 13830000, EGÚ Praha, 1994.
- [6] Aslanov I.V., Maksutenko S.N., Povkh I.L., Simonenko A.P., Stupin A.P. Izv.Acad.Sci USSR, Mech. zhidkosti i gaza, No.1, 33-43, 1980.
- [7] Gasljevic K., Matthys E.F. ASME Fluids Engng.Conf., Vol.2, July 7-11, San Diego, 1996.
- [8] Myska J., Zakin J.L., Chara Z. Appl.Sci.Res., 55, 297-310, 1996.
- [9] Rose G.D., Foster K.L. J.Non-Newt.Fluid.Mech., 31, 59-85, 1989.

Acknowledgement

This research was supported by Grant No. 103/95/0006 of the Grant Agency of the Czech Republic. The donations of surfactants by AKZO Chemical Co. and Hoechst AG are gratefully acknowledged.

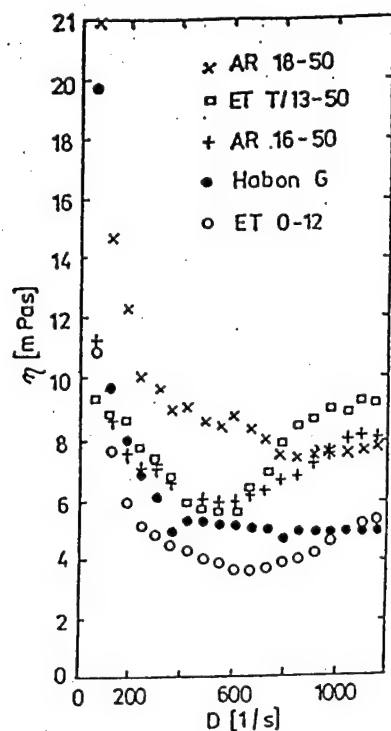


FIG.1

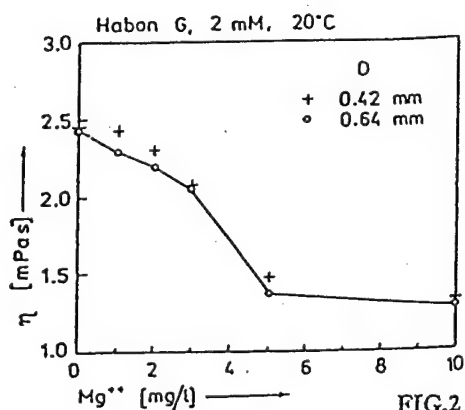


FIG.2

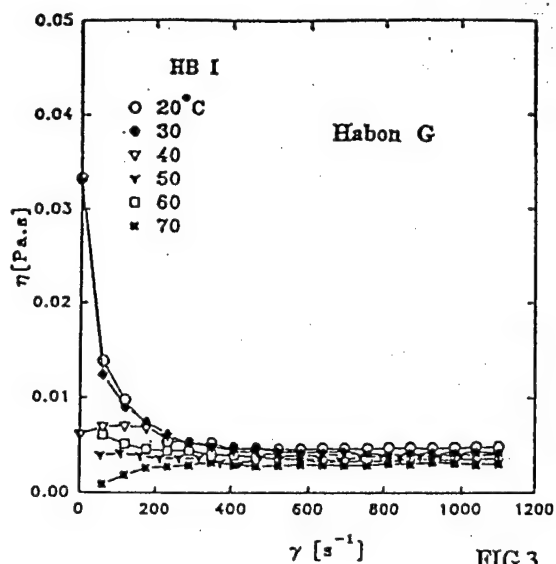


FIG.3

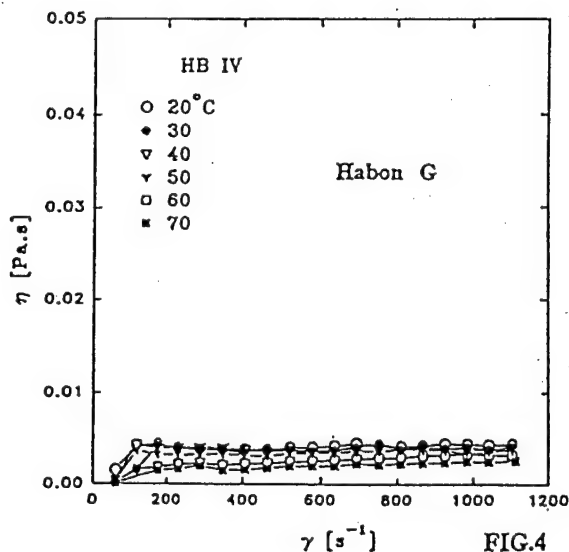


FIG.4

FIG.1 Viscosity curves of different surfactants at 20°C show similar pattern at low shear rates D where viscosity η reaches high values. Concentration of Habon G was 2mM, all other concentrations surfactant/sodium salicylate were 5/12.5mM. Measurements in Couette system were done on presheared samples under laminar conditions. The decrease from high values of η with increasing shear rate is seen in all samples.

FIG.2 The decrease of apparent viscosity as measured in capillary viscometers is influenced by Mg^{++} presence.

FIG.3 Temperature dependence of 2mM Habon G viscosity is seen in these measurements without preshearing. High values of viscosity at low shear rates γ are found in cooler solutions, Newtonian viscosity is found at all temperatures at higher shear rates.

FIG.4 The pattern of viscosity curves of Habon G solutions with 5mg/l Mg^{++} ($MgSO_4$). SIS is completely lost at all temperatures, Newtonian-like behavior at higher shear rates holds on, absolute values of viscosity are lower.

Velocity profile development behind an orifice plate in the drag reducing surfactant flow

Zdeněk Chára, Pavel Vlasák, Miroslav Severa

Institute of Hydrodynamics, Prague, Academy of Sciences of the Czech Republic

The paper deals with the investigation of the influence of a sharp edged orifice plate on turbulent characteristics in drag reducing surfactant flow. By LDA method the profiles of velocity and RMS values of water and surfactant solution of Habon-G were taken up to the distance $4D$ upstream and $96D$ downstream from the plate.

The experiments were performed in a closed recirculating hydraulic loop with horizontal glass pipe of inner diameter 39.4 mm. The description of the system can be found in [1]. The LDA system was derived from Dantec system 55X and for data processing Dantec Burst Spectrum Analyzer (BSA-enhanced) was used. The surfactant we used in the experiments was Habon-G - hexadecyl dimethyl hydroxyethylen ammonium 3-hydroxy-2-naphtoate (product of HOECHST Comp. FRG) at the concentration 0.095% and temperatures about 25°C .

Fig.1 shows a schematic diagram of the plate. The ratio of concentric hole diameter d to pipe diameter D was 0.5 ($\beta = 0.5$). The distances of pressure tap positions were $L_1 = D$ from the upstream face of the plate and $L_2 = D/2$ downstream from the plate. Pressure differences were measured by the differential pressure transducer Hottinger-Baldwin. Fig.2 shows plate pressure differences in dependence on mean pipe velocity. Due to the high unrecoverable pressure losses in this orifice plate the maximum available velocities were below 1.3 m/s that is 2.2 times less than maximum velocity we have measured for water in the same hydraulic system without the orifice plate and even 3.3 times less than maximum velocity for surfactant and hence the drag reduction effect in such hydraulic system with this type of the orifice plate is highly damped. As can be seen from Fig. 2, the experimental data of Habon-G though lie below the data of water alone, but the differences are very small (about 5%).

We have measured the profiles of longitudinal velocity component in two positions upstream ($4D$ and $0.35D$) and ten positions downstream from the orifice plate ($0.3D - 96D$). In the distance $4D$ upstream the velocity profiles of water and surfactant had a similar shape as we have measured in the pipe without the plate [1]. Due to the high shear rates in the entrance part of the orifice plate the micelle network (which is probably responsible for drag reduction effectiveness of surfactant) was broken up and the velocity profiles of water and surfactant were practically the same up to the distance $12D$ downstream. This situation is documented on Fig. 3, where two velocity profiles are shown. Since the flow is symmetrical, only halves of velocity profiles are drawn. In the distances between $7D$ and $12D$ downstream both velocity profiles were very flat. While the profile of water velocity rebuilt its primary shape after the distance $45D$ downstream, the profile of velocity of surfactant developed substantially slowly and there were perceptible differences in velocity profiles in the distances $82D$ and $96D$ and probably the distance $96D$, which was the maximum distance obtainable on our experimental loop, was not sufficient to develop the velocity profile in surfactant.

We have also measured the profiles of RMS (root mean square) values of longitudinal velocity component. In the distance $4D$ upstream the profiles of RMS had a similar shape as in the pipe without the plate. In the downstream vicinity of the orifice plate the course of RMS values was influenced by the sharp edge of plate. In the distance $1.35D$ downstream the surfactant RMS values were higher only around the orifice edge, but in the distances $4.8D$ and $7D$ the RMS values in surfactant were higher in whole profile of the pipe. On Fig. 4 the RMS values in distances $1D$ and $4.8D$ downstream the plate are plotted. In the distance $12D$ both RMS

profiles were practically the same. In the distances $32D$ and $45D$ the surfactant RMS values were in a near wall region higher, but very quickly decreased below the water line and they were very flat. In the larger distances the surfactant RMS values decreased and approached the water points in a near wall region and more gently dropped below water line. Also from the RMS profiles the developing of surfactant flow over the distance $96D$ downstream the orifice plate was obvious.

Acknowledgement

This research was partially funded by the Grant Agency of the Czech Republic under No. 103/94/1186.

[1] Chára, Z., Zakin, J.L., Severa, M. and Myška, J.: Turbulence measurements of drag reducing surfactant systems, Experiments in Fluids 16, 36, (1993).

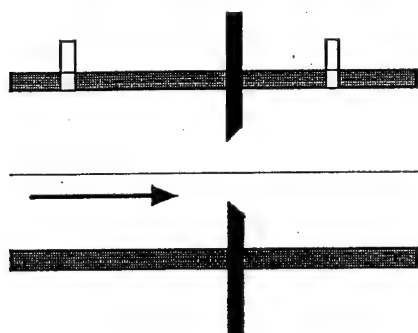


Fig. 1

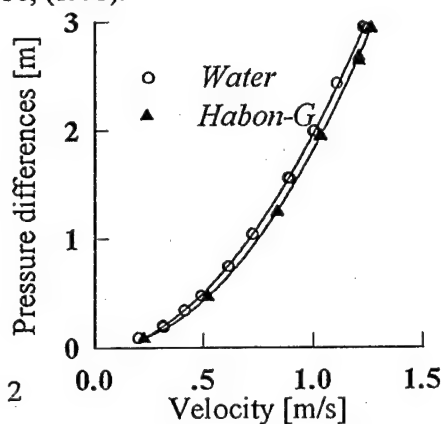


Fig. 2

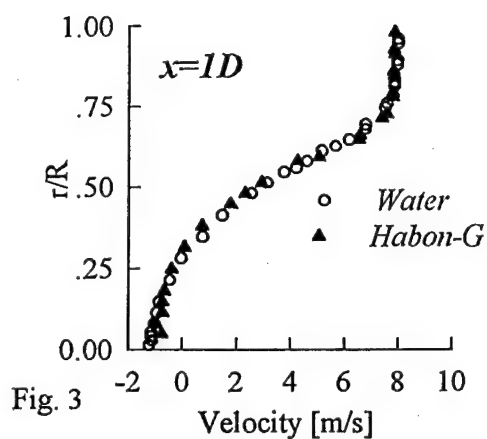


Fig. 3

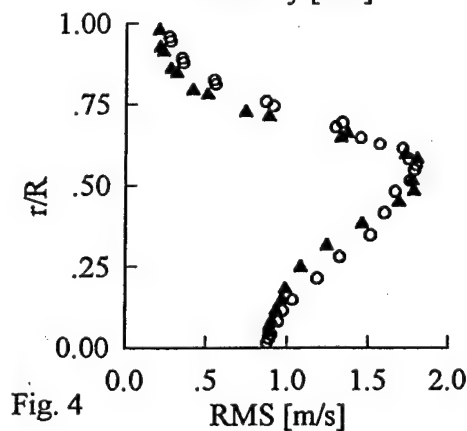
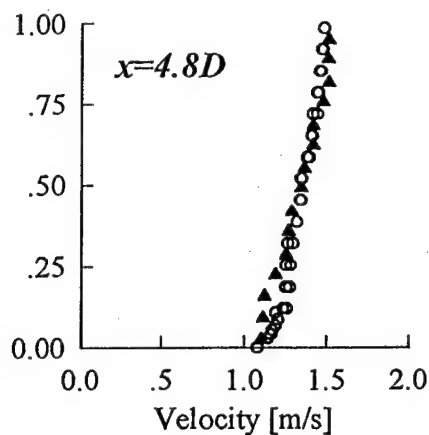
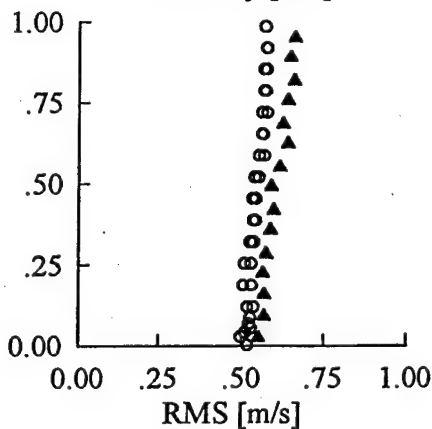


Fig. 4



Effect of a drag reducing polymer solution in the free turbulence confined by a tip vortex

**Daniel H. Fruman
Jean-Yves Billard**

Tip vortices are very peculiar structures showing intense turbulence in the core (viscous region) as compared to the free stream and potential region levels. Experiments conducted injecting a drag reducing polymer solution at the tip of an elliptical wing have shown significant modifications of the radial distributions of the velocities, higher moments and cross products. By analyzing the results it is shown that the effect of the polymer solution is to nearly eliminate the turbulent velocity fluctuations. The reasons for such a behaviour are discussed and their impact on the interpretation of wall turbulence damping by DR polymer additives is analyzed.

SESSION 3:

BIOLOGICAL ASPECTS

(Thursday Afternoon)

Aerodynamic studies of starling models: Wing - trunk - interferential drag effect and surface roughness.

F. Wedekind, R. Gesser, R. Kockler & W. Nachtigall
FR 13.4 Zoologie, Universität des Saarlandes, D-66041 Saarbrücken

Material and method:

Full scale artificial resin models (with detachable wings) of a starling gliding in a wind tunnel were built for aerodynamic studies (fig.1). The basic model has a smooth outer surface, the relatively sharp leading edges of beak, wings and tail, induce a turbulent boundary layer.

By means of a very sensitive two-component balance with an air-cushioned load transmitter, which is installed under the open measuring area of a wind tunnel, lift and drag forces are measured at different angles of attack at a wind speed of 8 m s^{-1} .

Force measurements can be carried out on complete models, or models with or without tails. For interferential drag measurements, the wings are placed by means of a separate support, as close and as naturally as possible to the trunk thus changing the flow around it indirectly. Changes in trunk forces are registered without measuring the forces of the wing. Model trunks with and without tails are compared.

The surface roughness of individual wing models mounted on a spindle-shaped support was studied (fig 2).

Results:

Interferential drag:

Lift and drag created by the trunk is greatly influenced by the close presence of the model wings. With wings, but without a tail, the trunk develops more lift throughout a large range of angles of attack than without wings (fig 3b). At low angles of attack, the total drag of the trunk is reduced by negative interferential drag, and the minimum drag decreases by 54% ($C_{D,\min}$ of the trunk alone is 0.08). The tail appears to lie in the higher range of angles of attack in the downwash of the wings, where interferential drag has little effect on the total drag of the trunk (fig. 3a). Nevertheless, the tail creates considerable lift. In a natural flight position (8° gliding angle, 8 m s^{-1} wind speed), the trunk with tail produces almost 26% of total lift (Wedekind et al. 1996).

Wing roughness:

Compared to smooth wings, the model wing with a layered surface (roughly comparable to the feather arrangement) produces more lift over a larger range of angles of attack. So, at a given lift, drag is reduced indirectly (fig 4). With an even finer surface structure, similar to that of a fine feather composition, drag could not be reduced any further as yet.

Discussion:

It appears that the turbulent flow around the wings of a model starling can be positively influenced by relatively large irregularities (layer thickness $0.2\text{-}0.5\text{ mm} \approx 2.3\text{-}5.9\%$ of maximum wing thickness), which also reduces the breaking loose effect of flow. The extent to which the position of the layers in relation to the direction of flow influences the drag must still be studied.

Our measurements suggest that the layered wing surface also has an influence on the interferential drag between wings and trunk and may even reduce it.



fig. 1: Model of a gliding starling.

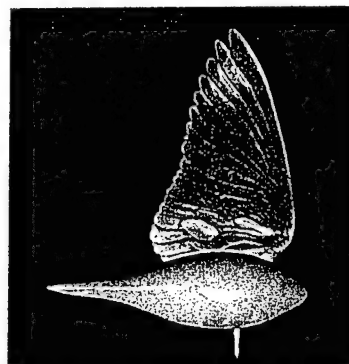


fig. 2: Model wing, with feather-like layers, mounted on a spindle.

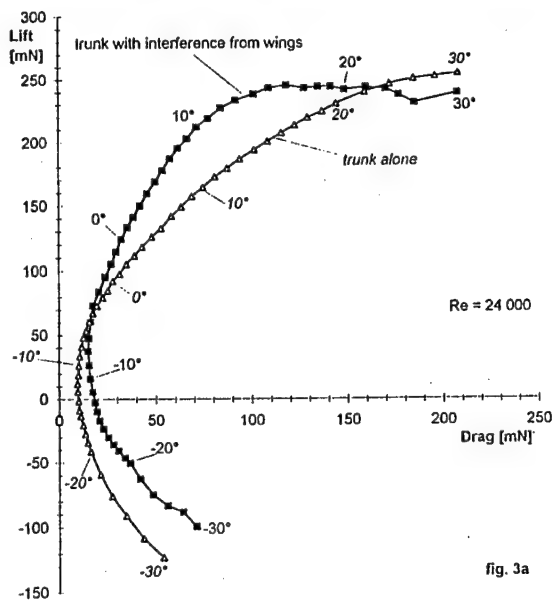


fig. 3a

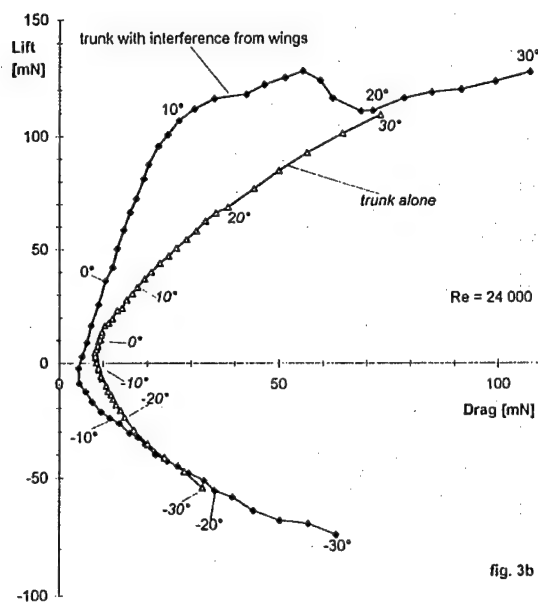


fig. 3b

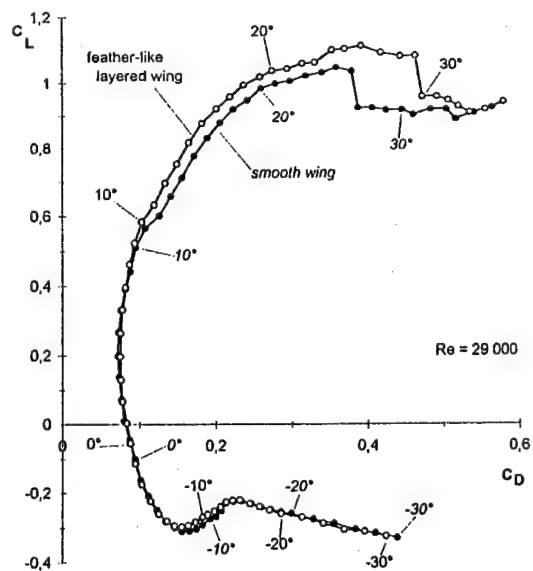


fig. 4

fig. 3: Change in lift and drag, due to wing interference, a: Trunk with tail, b: Trunk without tail.

fig. 4: Polar diagram of a smooth and of a feather-like layered wing. C_L and C_D are relative to wing area.

Reference:

F. Wedekind, R. Gesser, R. Kockler & W. Nachtigall 1996: Verh. Dtsch. Zool. Ges. 89.1, 228, Fischer Verlag.

Flexible flaps for separation control on a wing with low aspect ratio

Patone, G. & Müller, W.

Techn. Univ. Berlin, FG Bionik & Evolutionstechnik

As part of a bionics project, an airfoil (NACA 2412) has been tested for its stall behaviour with flexible flaps attached to the upper surface. Analogous to the cover feathers on a bird's wing, the flaps are able to prevent or at least delay the spreading of the eddy from the trailing towards the leading edge of the wing during stall. The experiments were conducted in an open circuit wind tunnel at $Re=120\ 000$, with the airfoil having an aspect ratio of 3.5. The NACA 2412 exhibits a sudden drop in generated lift when the angle of attack is increased beyond the critical value. With the appropriate flaps attached, this drop in lift production can be prevented or at least delayed, as the flaps will be lifted off the surface automatically when flow separation commences. It is important to note that the flaps remain smoothly on the surface of the airfoil as long as the angle of attack is below the critical value. Therefore, they have nearly no negative effect on the drag. Best results were obtained using materials of a certain porosity and flexibility. Because of the low aspect ratio of the airfoil used, the flow separation starts from the centre of the airfoil, and thus it is crucial that the flaps can form a pocket. So these flaps can serve as a smart safety device. In order to gain better insights into the aerodynamic mechanism of the flaps, the pressure distribution over the surface of the airfoil was investigated. The results show the effect of the flaps to be a restriction of the separation, so that the remaining part of the airfoil can still generate lift.

Swordfish rostrum as a generator of vortices, reducing hydrodynamical drag

V.I. Merculov

Institute of Theoretical and Applied Mechanics,
Siberian Branch of the Russian Academy of Sciences.
630090, Novosibirsk, Russia.

L.I. Maltzev

Institute of Thermophysics, Siberian Branch
of the Russian Academy of Sciences.
630090 Novosibirsk, Russia

Dr. Rudolf Bannasch

Technische Universitat Berlin
Fachgebiet: Bionik und Evolutionstechnik
13355 Berlin Ackerstr. 71-76
Germany

ABSTRACT

Swordfish, sailfish, marlin are most speedy sea inhabitants. Their maximal speed has a record as high as one hundred kilometres per hour. Fishes like these usually have a long spear-like bone (rostrum) which ranges up to one third of the body length. Biologists advocate that this body part can not be used for attack or defence. We analyse a hypothesis that this spear is a generator of helical vortices that reduces the hydrodynamical drag. The report contains a mathematical model for flowing of slender long body with a rough surface. The half-infinity slender body with one-scale roughness was taken as a body model. The known stability of axisymmetrical flow along the slender body allows to regard that the disturbances in flow are generated only one-scale roughness of the body surface. The solution of Reynolds equations for averaged turbulent flow, which are enclosed by length mixing model (for the given case the length mixing is constant that equal to the roughness scale), allows to define the profile of averaged velocity. Contrary to the laminar profile, the resultant profile of averaged velocity is instable for helical disturbances. The Orr - Sommerfeld equation for disturbed flow (here the flow is free of molecular viscosity and have turbulent viscosity with known scale) allows to obtain eigenfunctions in the form of helical disturbances and eigenvalue which defines the phase velocity and increment disturbance. The developed helical vortices reconstruct a common boundary layer with sliding of liquid layers and with big velocity gradients on a fish's body into the flow with rolling vortex, which has a small velocity gradient and, thus, a low hydrodynamical drag. The experimental study of water flow along the slender long rough body verified the formation of helical vortices in the wall flow.

Numerical Analysis of Penguin Hydrodynamics

**P. Kolobov, B. Kolobov,
L. Maltzev, R. Bannasch**

The report contains:

- the method of calculation of potential flowing of axisymmetrical body
- the method of calculation of laminar-turbulent boundary layers on axisymmetrical body
- appropriate data on penguins

**The measuring devices as microfabricated pressure sensores for
investigation of dolphins' boundary layer.**

E. V. Romanenko

*A. N. Severtsov Institute of Ecology and Evolution RAS, Leninsky
prospekt 33, Moscow, 117071, Russia.*

There are elaborated some constructions of pressure pulsation measuring devices for investigation of the thin structure of the boundary layer on the body of the free swimming dolphin. The sensitive elements of the all above constructions are the piezoelectric ceramic done in the form of rod or plate with two silver electrodes. The transverse size of the rod and the plate is approximately 1 - 2 mm. The length is about 10 mm. The sensitive element is mounted in the metal cilindric holder with the dia 2 - 5 mm and it is connected by the thin screened conductor with electronic amplifier and with the recording device.

Using such pressure pulsation measuring devices the distribution of the levels of turbulence has been investigated across the thickness of the boundary layers of the dolphin, scales and spectrum of the turbulence, autocorrelating and cross-correlating characteristics.

Experimental investigations on the boundary layer development in swimming penguins: mechanisms of drag reduction and turbulence control

Dr. Rudolf Bannasch
Technisch Universitaet Berlin
Bionik und Evolutionstechnik (ACK1)
Ackerstrasse 71-76
D-13355 Berlin, Germany

Tel. and Fax: +49 30 31472658
e-mail: bannasch@fb10.tu-berlin.de

ABSTRACT

More than forty Million years ago, penguins have changed from aerial to fast and sustained underwater flight exclusively. One can assume that in tens of million generations exposed to selection under the most extreme conditions on the earth, nature has found an optimal solution to the energetic problem involved. The solution includes maximum efficiency of the wing-propulsion system as well as drag reduction. Experimental studies conducted on live penguins as well as measurements with life-sized models of these birds in a water tank revealed extremely low drag coefficients, although there was some evidence that transition from laminar to turbulent near-wall flow occurred in the most frontal part of their body. At higher Reynolds numbers they were 20 - 35 % lower than those reported for the best turbulent technical bodies. Contrary to fish and dolphins, the penguin's trunk does not contribute to thrust production. Trunk oscillations during a wing beat cycle are moderate. Therefore, the spindle-like penguin trunk may well serve as live example for how energy may be saved by shape optimisation of relatively short and thick stiff bodies offering a large volume with minimum drag. Using the arithmetic means of normalised data on body geometry from three medium sized penguin species, an axisymmetric body was built. By drag measurements in a water tank, this body of revolution was found to be an excellent low-drag laminar body (e.g. the lowest frontal drag coefficient was $c_{Df} = 0,0156$, measured at $Re = 2,331 \cdot 10^5$ with the maximum diameter as reference length). When the transition from laminar to turbulent flow was triggered at the beak (at 5 % of the body length), this technical body showed nearly the same drag characteristics as observed in the original penguin models. Most surprising, in the turbulent case the drag coefficients remained even lower than those of a turbulent flat plate of equal length. Moreover, the decline of the drag coefficients with increasing Reynolds numbers was steeper for all penguin bodies than for the flat plate. Detailed studies on boundary layer development suggested that drag reduction resulted from the wave-like outlines of the body. Contrary to the flat plate and also to technical bodies, a stepwise pressure and velocity distribution was found along the contour of the axisymmetric "penguin body" with alternating concave and convex parts. Following high acceleration at the convex tip of the beak, the thickness of the boundary layer suddenly increased over the concave part at the end of the beak and remained nearly constant downstream until the maximum diameter of the body was reached. Due to repeated acceleration at a nearly constant rate (stabilisation of the near-wall flow) over the convex parts interposed by sections with nearly constant flow velocity (concave parts of the contour), the turbulent velocity fluctuations within the boundary layer were kept at a quite low level until the end of the body. Consequently, also the wall shear stress (friction) was kept low. Hypothetically, by this mechanism the vertical exchange of energy can be managed in a way that the boundary layer receives energy from the outer flow just sufficient to prevent flow separation. Unfortunately, in these experiments the influence of

the compliance of the original penguin plumage and of the riblet-like microstructure of its surface could not be investigated. However, during our last Antarctic expeditions, more sophisticated hydrodynamic studies were carried out on live penguins swimming in a special still water tank. For this purpose, a novel method for flow visualisation in live animals with controlled dye ejection underneath of the plumage was developed. In combination with conventional video and high-speed video analyses, fundamental insights into the details of the boundary layer development at various flow conditions and into its interaction with the vortex system generated by the wings could be obtained. The most impressive sequences will be shown in the video presentation. These visualisation experiments confirmed that, in fact, transition occurred in the most frontal part of the bird's body. However, the boundary layer did never become "chaotic" further downstream. In most cases, a quite regular wavelike pattern (wave length 2 -3 cm with only the amplitude increasing towards the end of the body) was formed. With a velocity of approx. 95 % of the swimming speed, the waves appeared to be nearly stationary in the fluid. Corresponding to the wing circulation changing its direction during each stroke phase, the waves became more pronounced on the dorsal and ventral side during the up-stroke and down-stroke, respectively. Apart from passive mechanisms (multiple curvature effects, compliance and microstructure of the plumage) possibly responsible for keeping boundary layer turbulence at a certain but overall low level, it will be shown in the video demonstration that (and how) the structure of the near wall flow can be managed also by a number of active mechanisms. Tiny adjustments of the body shape (changes in the position of the head, neck, feet and tail) and thereby of the pressure and velocity distribution had a remarkable influence on that flow pattern. Additionally in some cases, just after descending, some parts of the body became covered by a thin film of air that reduces the wall shear stress locally to an absolute minimum. These areas corresponded well to those characterised by a low pressure gradient in the earlier model experiments. For the most part, the air was squeezed out of the plumage. The most persistent air bubble was the one in the neck, which was frequently renewed obviously by exhalation and subjected to unsteady oscillation. At this location a vortex seems to be formed which is assumed to underlie the same oscillation. This could be a possible explanation for the mechanism generating the running wave observed further downstream in the boundary layer. Finally, an extraordinary measure to drastically reduce body drag temporarily could be a sudden ejection of large amounts of air bubbles by the bird. This can be observed when the animals try to achieve extreme acceleration e.g. during escape reactions or before jumping out of the water. Thus, the presented material provides a number of new fundamentals for the understanding of viscous drag reduction in nature and for a large variety of possible applications in engineering.

SESSION 4:

CONTROL OF TRANSITION, TURBULENCE AND SEPARATION

(Friday Morning)

Active control of TS waves

G. Pailhas, G. Casalis, J.L. Gobert

ONERA-CERT

2, Av. Edouard Belin 31055 Toulouse-Cedex

The natural instabilities of flow which appear on aerospace vehicle surfaces are a source of energy dissipation increasing the drag and producing noise and vibrations, therefore they have prejudicial consequences on the performances.

In the present study, we consider the so-called Tollmien-Schlichting waves which are the primary instability leading to the transition from laminar to turbulent flow. The main goal is to get a better understanding of the mechanism driving the TS waves in order to propose in the future a technique to cancel or at least of considerably reduce them as soon as they start to grow.

TS wave cancellation is a quite complex problem and for that reason, it has been decided to proceed gradually and to increase progressively the difficulties step by step.

The first phase was to develop a system able to cancel a *monochromatic wave* on a flat plate with a zero pressure gradient. It was proposed to use the wave superposition principle. A counter disturbance is applied at a given point with the frequency of the monochromatic wave and the appropriate phase and amplitude in such a way that the resulting signal will be zero.

A disturbance generator using a piezo-electric element has been developed to produce the required monochromatic Tollmien-Schlichting wave. This generator has been installed on a flat plate in a small research windtunnel and tested with a flow speed of 12 m/s^{-1} . The first work was mainly to compare experimental results with the stability theory in order to check whether the disturbance generator produces a Tollmien-Schlichting wave or not.

The implementation of a second generator working as actuator to cancel the TS wave has been tested. The verification of the principle of wave superposition has been achieved.

Qualification of hot film sensors, flush with the flat plate surface, providing the relevant informations to perform the closed loop control, is in progress.

As longer term action, the case of natural Tollmien-Schlichting waves is considered, this will require to solve the difficult problem of controlling wave packets.

PRESSURE DRAG REDUCTION CONCEPTS FOR MANEUVERING SUBMARINES

Saeed Farokhi*, Ray Taghavi**
The University of Kansas
Aerospace Engineering Department
Lawrence, KS 66045

&

Ronald Barrett*
Auburn University
Aerospace Engineering Department
Auburn, AL 36849

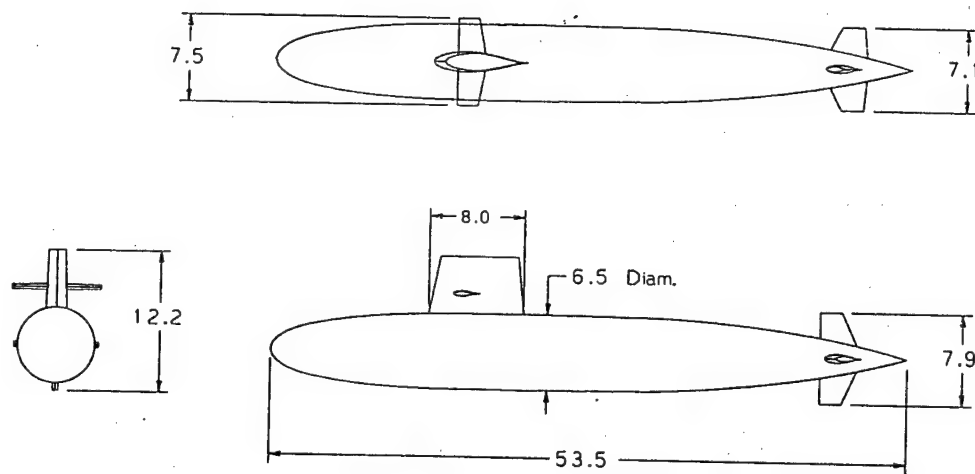
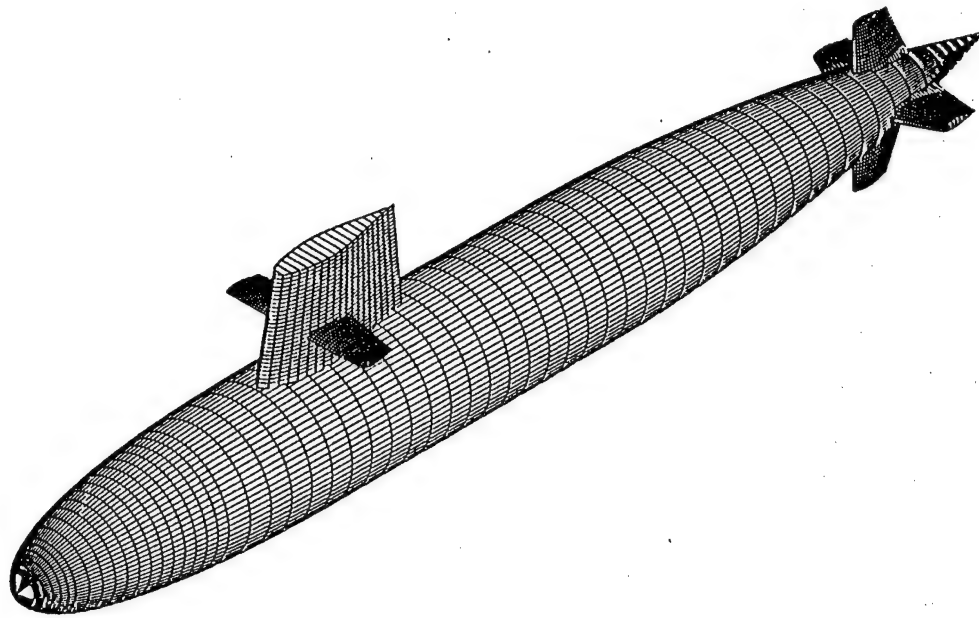
ABSTRACT

Innovative concepts in smart tetrahedral vortex generators (STVG) are developed and applied to bodies of revolution, e.g. a submarine geometry. The STVGs in flush (stowed) position offer the advantage of nearly eliminating the increment of pressure drag due to the vortex generators, $\Delta C_{D, VG}$, or simply ΔC_{D0} . The deployed position of STVGs will create pairs of streamwise vortices capable of flow attachment. A maneuvering submarine at high angles of attack and yaw experiences massive flow/vortex separation on the leeward side of the hull and the sail. An elementary model of this flow environment, in fluid mechanics, is a yawed cylinder in cross flow. The massive wake generated by a maneuvering submarine is the cause of significant pressure drag and this in turn prevents the desired agility expected of an attack submarine and will increase its acoustic signature. A distributed flow sensor(s) and actuator(s) in conjunction with a central processor, making up the elements of a smart vortex management system, is then capable of detecting the flow separation and using a proportional-deployment control algorithm, the actuators are able to minimize the extent of the flow separation. A scaled model of an attack submarine (134 cm long, 0.1215 fineness ratio) is tested in a 91.5 cm x 122 cm subsonic wind tunnel at high angles of attack and yaw (see Figure 1). Surface oil flow visualization and the fluorescent paint techniques were utilized in the experiments. Surface streaklines show a very strong vortex separation behind the submarine sail and a large three-dimensional separation zone on the leeward side of the submarine without the VGs (see Figure 2). A trace of the surface streak pattern is also shown in Figure 3 identifying a stagnation point horseshoe vortex on the sail as well as other 3-D vortex separation boundaries. The model was subsequently tested with the fixed VG devices installed and the large vortex separation region was virtually eliminated (see Figures 4-6). These remarkable results, although qualitative at this time, were obtained with no optimization of device height and/or spacing; yet tremendous effectiveness was demonstrated. Four conceptual designs of smart vortex generator systems suitable for blunt body flow management in yaw are also presented in Figure 7. The schematics of a multi-hinge STVG in stowed and active mode is shown in Figure 8. Additional results on surface flow visualization will be presented at the Working Meeting in Berlin.

*John E. & Winifred Sharp Professor

**Associate Professor

*Assistant Professor



All Dimensions are in Inches

Figure 1. Isometric and three-view of the attack submarine under investigation.

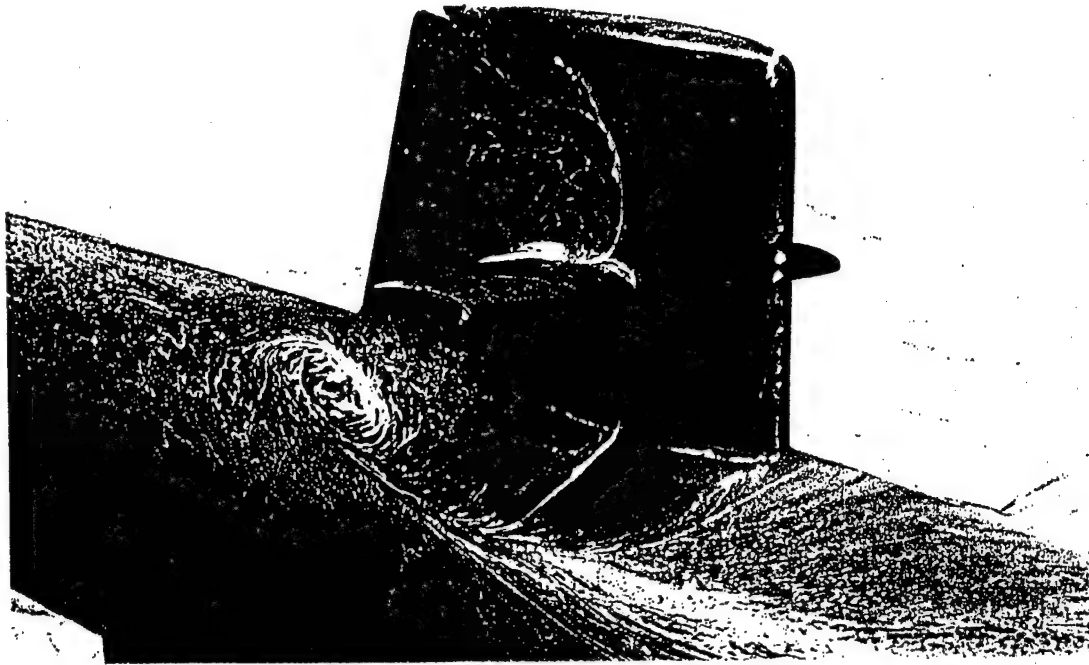


Figure 2. Surface oil flow visualization

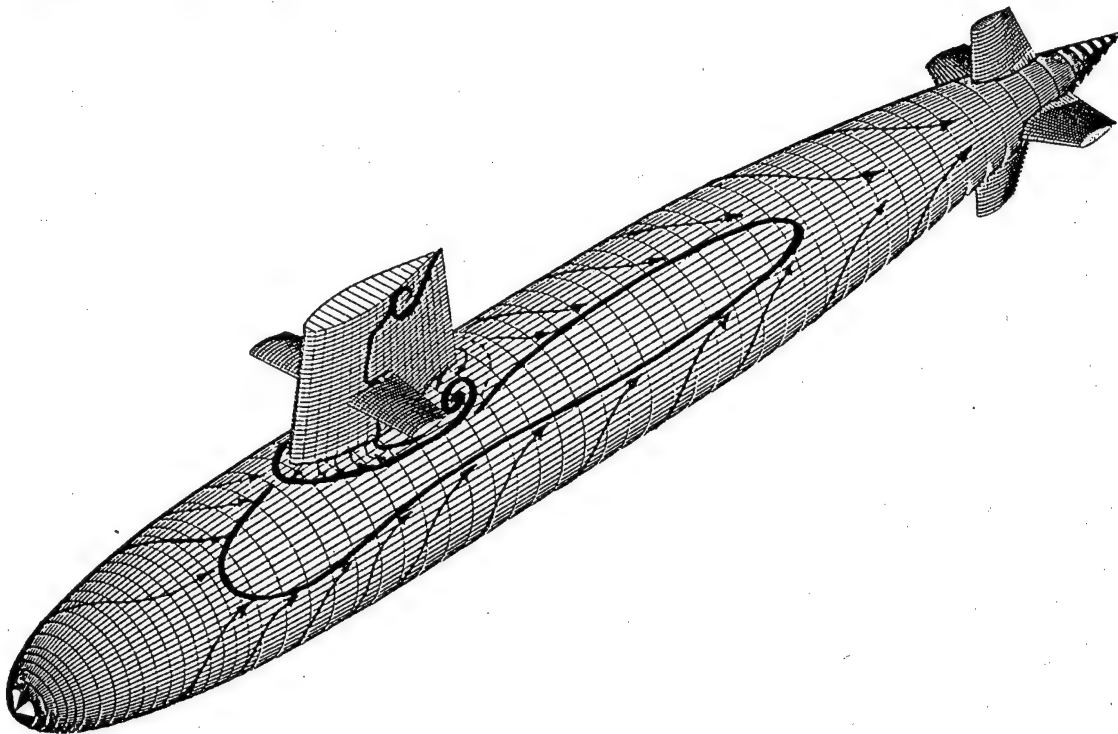


Figure 3. Trace of 3-D separation pattern and surface streaklines

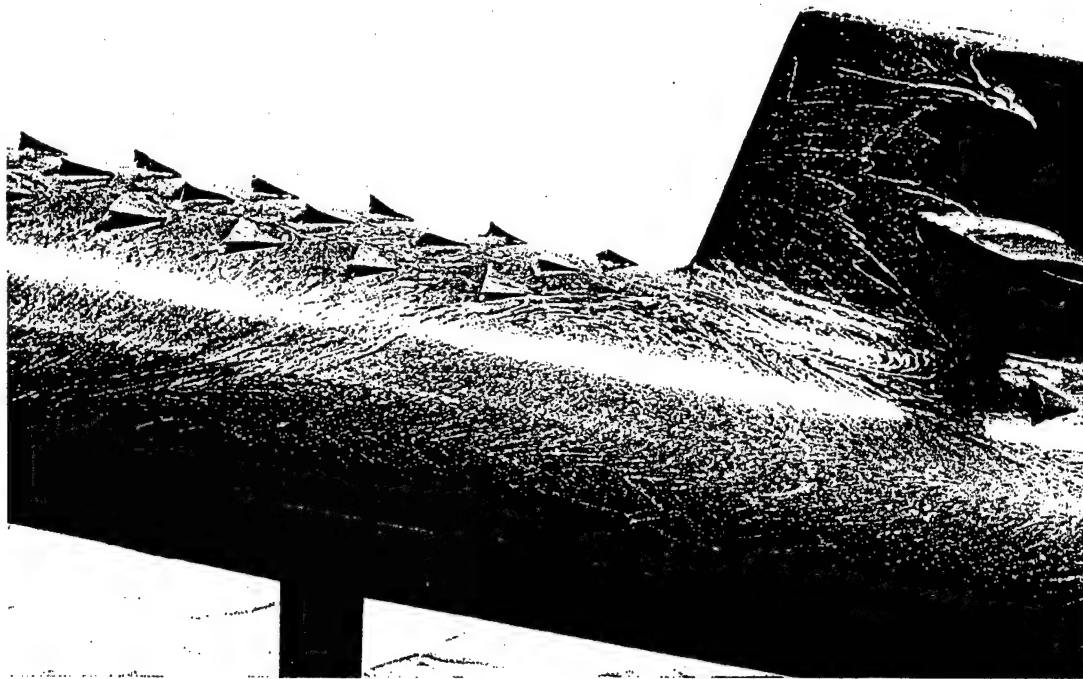


Figure 4. Submarine sail and aft hull flow visualization with fixed STVGs.

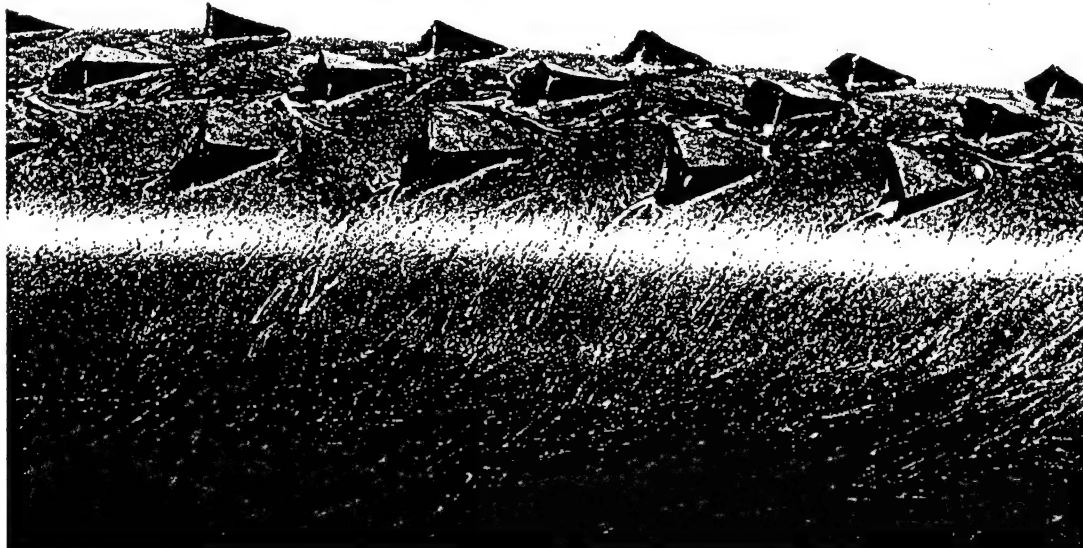


Figure 5. Close-up view of surface streak pattern on a submarine hull with distributed, fixed, non-optimized STVGs.

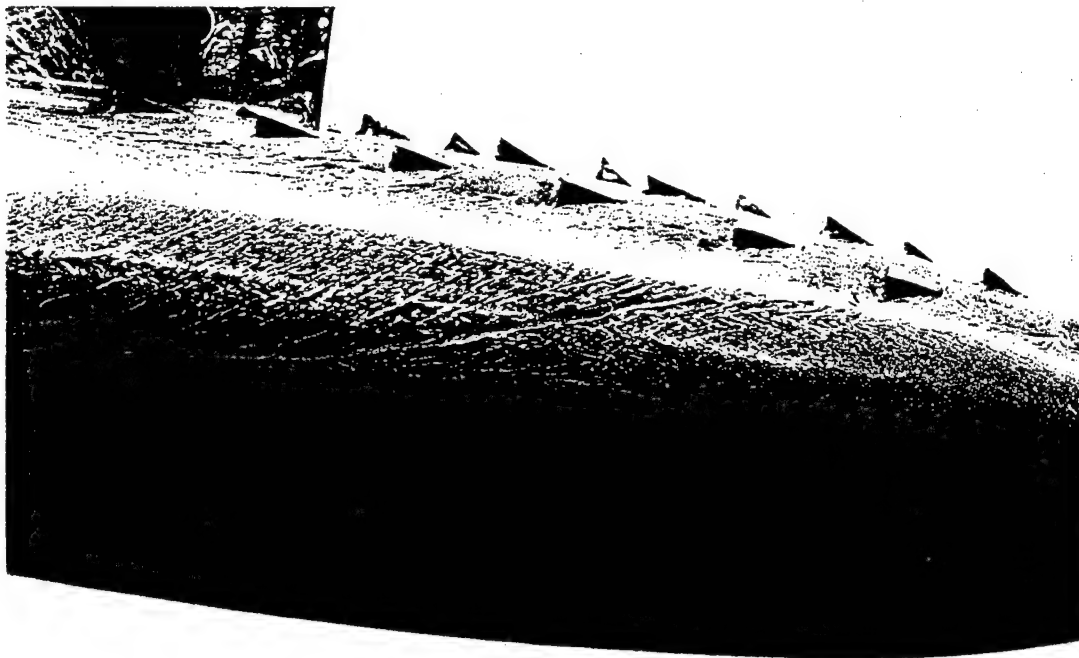


Figure 6. Surface flow near the blunt nose with non-optimum, fixed STVGs.

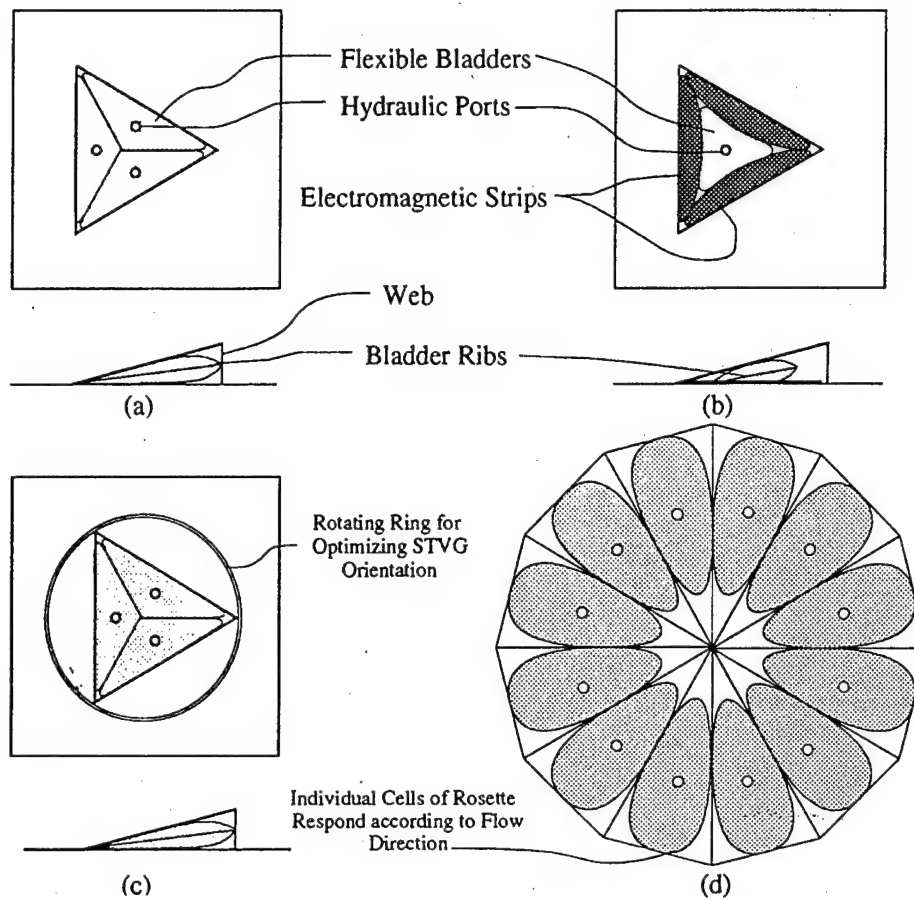


Figure 7. Four concepts in variable-hinge smart tetrahedral vortex generators

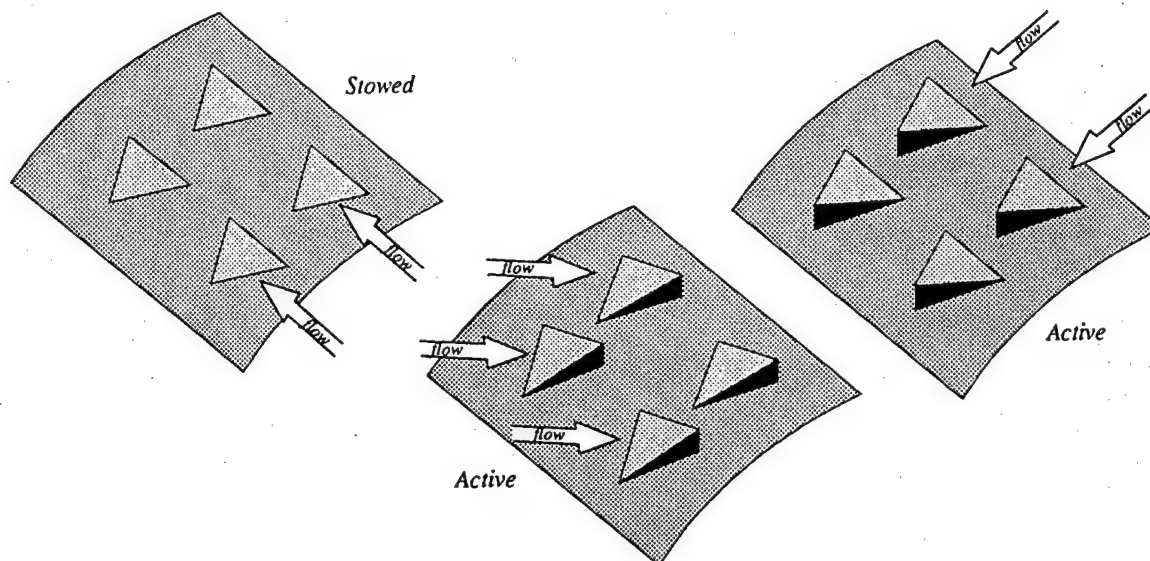


Figure 8. Multi-hinge STVG response to flow angularity

Turbulence diffusion mechanism on active deforming surface.

Voropaev G.A

Institute of Hydromechanics, National Academy of Sciences of Ukraine

Turbulent boundary layer over rigid smooth surface have been investigated good enough, in spite of this region of turbulence is inhomogeneous and essentially anisotropic even for microscales. Energy balance in each point of the turbulent boundary layer is determined by statistic velocity and pressure within some neighbourhood of this point. This neighbourhood range and shape (correlation scale magnitudes along different directions) depends on integral value $Re=U_0\delta/\nu$ not so much as this point location about the streamlined surface, i. e. the local Reynolds number $Re=u_*y/\nu$.

$$\frac{1}{2} \frac{\partial v_j^2}{\partial t} = -v_i v_k \frac{\partial U_i}{\partial x_k} - \frac{1}{Re} \frac{\partial v_i}{\partial x_k} \frac{\partial v_i}{\partial x_k} + \frac{\partial}{\partial x_k} \left[-\frac{1}{2} v_j^2 v_k - p v_k + \frac{1}{Re} v_k \frac{\partial v_k}{\partial x_k} \right] \quad (1)$$

All the terms in the turbulence energy balance equation (1) are important in the closest region to the wall, among them the terms describing turbulent and viscous diffusion of fluctuate energy

In the boundary layer over a rigid smooth surface, fluctuate energy flux directs from the point where $k=k_{max}$ ($y^+ \approx 18$) as towards the surface and away from the surface. The flux directed away from the wall is small by magnitude. The flux variation leads to an additional turbulence energy source near the wall $0 \leq y^+ \leq 5$ and additional dissipation in the region $5 \leq y^+ \leq 30$.

In the boundary layer over an absorbing surface, when energy of the oscillating surface may be neglected, there is a qualitative analogy with boundary layer over rigid smooth surface at lower level of turbulence energy intensity.

The fluctuate energy flux grows near the deformable surface at $k|_{y=0} \neq 0$ for account of viscosity, but when moving far from the wall, it becomes less than that in boundary layer over the rigid smooth surface. This flux diffusion leads to sudden growth of turbulence energy production near the wall at $0 \leq y^+ \leq 2$, as well as dissipation increases by 2÷3 times in the region $2 \leq y^+ \leq 8$ as compared with turbulent boundary layer over the rigid smooth surface. The difference of this two flows is not noticeable farther from the wall.

In a case of such active surface deformation when the surface wave length is small in comparison with the boundary layer thickness ($\alpha \gg 1$), and certain phase shift between maximum energy-carried disturbances and surface displacements, as well as certain phase speed of surface deformation, there are created such velocity fluctuation in the boundary layer which provided negative diffusion near the surface. As a result, the minimum turbulence energy point becomes equivalent to the point placed on the surface when a rigid smooth surface is streamlined. It means that maximum turbulent stress region moves away from the surface.

The turbulent transport of kinetic energy $\left(\frac{\partial}{\partial y} (-\overline{v_2 k}) \right)$ and turbulence pressure energy

transport $\left(\frac{\partial}{\partial y} (-\overline{v_2 p}) \right)$ in the near-wall region may be associated with turbulence energy gradient.

As experimental data have shown, turbulence kinetic energy diffusion and pressure fluctuation energy are equal approximately and exceed by modulus both production and dissipation in the near-wall region of turbulent boundary layer over rigid smooth surface. But they have different signs. Pressure diffusion is more then kinetic energy diffusion at $0 \leq y^+ \leq 12$, and at contrary at $12 \leq y^+ \leq 40$. Then their sum gives additional production at $12 \leq y^+ \leq 40$ and dissipation at $y^+ > 12$. Destruction of the balance between these mechanisms of turbulence energy transport can lead to essential changes in the near-wall turbulence structure.

Effects of Acoustic Excitation on Flow Separation from a Wing at High Angles of Incidence

by

F.-R. Grosche and V.V. Kozlov

This paper concerns wind-tunnel experiments on the control of three-dimensional separation from a wing by external acoustic excitation.

Flow visualisation techniques were used to study the influence of sound waves on the flow separation from a wing of low aspect ratio 3:1 at Mach numbers $M \leq 0.1$. Tests were made within the Reynolds number range $6 \cdot 10^5 \leq Re \leq 1.2 \cdot 10^6$, at angles of incidence up to 25 degrees and yaw angles up to 30 degrees.

Two different configurations of the acoustic excitation have been applied:

1. Spherical sound waves from a loudspeaker within the acoustic far field
(Global excitation)
2. Sound waves focused by an elliptical mirror on a small region of the wing
(Localised excitation)

The experimental results demonstrate that acoustic excitation in a suitable frequency range can reduce the flow separation, which occurs at high angles of incidence all along the leading edge, to a much smaller turbulent separation region that mainly affects the central part of the wing.

Flow visualisation at different angles of incidence, yaw angles and Reynolds numbers reveals the three-dimensional structures and the unsteady characteristics of both types of flow separation.

The tests with acoustic waves focused by an elliptical mirror on a small part of the wing give some insight into the dependence of the spanwise structure of the separation on the position of the excitation region. An optimal position, where the effect of the sound is greatest, could be located.

We made video-recordings of the flow visualisation studies which present the characteristic flow features obtained with global and localised acoustic control of the leading edge separation. A short version of this video will be shown at the meeting.

THE FLOW TURBULISATION BY EXTERNAL ACOUSTIC FIELD AND HEAT TRANSFER ENHANCEMENT IN LAMINAR GAS FLOW

Harri KÄÄR, Toomas TIIKMA
Tallinn Technical University

Abstract

In this paper some heat enhancement phenomena appeared in laboratory test rig for investigation the gas combustion in auxiliary acoustic field are discussed.

The test rig consists of a gas burner 5 kW_{th}, low frequency sound generator, combustion chamber and in it exit flue gas duct, where located calorimetric probe for measuring the heat transfer efficiency. The laser-Doppler anemometry was used to determine the local flue gas velocities and the rate of turbulisation in the gas duct. Gas and air supply and flue gas content were measured. The temperature difference between water supply and outlet of calorimetric probe is measured by differential thermocouple, also the water flow rate is measured. The flue gas temperature is measured by a little suction pyrometer, combined with the gas analyse probe. This data give opportunity to estimate the heat absorption by probe and to calculate the heat transfer coefficient from flue gas flow to probe. Some data on heat transfer coefficient by convection are presented in Fig.1. The flue gas temperature about 300°C and the intensity of sound field up to 130 dB.

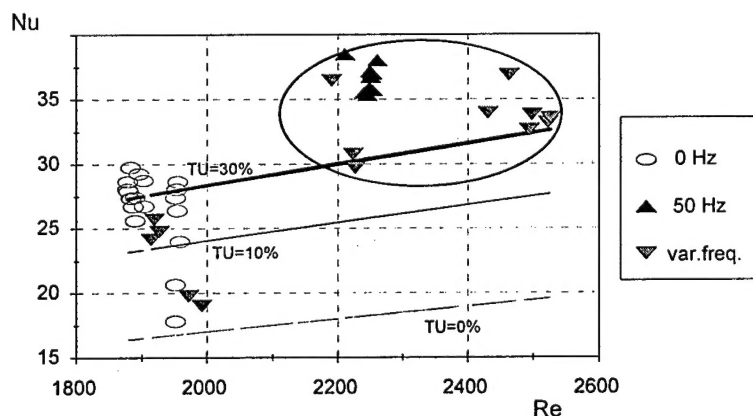


Fig.1. Heat transfer coefficient of calorimetric probe. Surrounded by ellipse area presents the data at sonic field. The lines represent the theoretical $Nu=f(Re)$ relationship (Eq. 1) at different rate of flow turbulisation.

$$Nu = \frac{\alpha \cdot d}{\lambda} = 0.26 \cdot Re^{0.6} \cdot Pr^{0.37} \cdot \left[1 - \left(\frac{d}{H} \right)^2 \right]^{0.8} \cdot Tu^{0.15} \quad (\text{Eq. 1}),$$

where d - outer diameter of the probe; H - width of the flue gas channel; Tu - the rate of turbulisation-of the gas flow, %.

The results of measuring heat transfer coefficient show that in external low frequency acoustic field takes place the enhancement of heat transfer probably due to the destruction of boundary layer by generated turbulence.

SESSION 5:

**LONGITUDINAL VORTICES
AND TWO-PHASE FLOWS**

(Friday)

H. Zondag and J.H. Voskamp
Eindhoven University of Technology
Department of Physics
P.O. Box 513, Eindhoven
The Netherlands
e-mail: jan@tnl.phys.tue.nl

Abstract: Drag reduction and hairpin vortices

Presentation: ca.10 minutes

The drag reducing effect of riblets has been discovered about 15 years ago and since then many papers appeared trying to explain the phenomenon or trying to optimize the shape of the riblets. Most of the work has to a certain extent an empirical character and we do not have the impression that the drag-reducing phenomenon is fully understood. This was one of the reasons to start a combined experimental and numerical study to the role of hairpin vortices in wall turbulence. Artificial hairpins were created in a laminar boundary layer both in a wind tunnel and in a water channel. In the wind tunnel extensive measurements have been carried out with an array of (single) hot wires, while visualisation studies were performed in the water channel. Each of these methods only provides incomplete information. However, the combination of the investigations leads to more certainty about a number of results.

Hairpin vortices are created by means of a hemisphere-type obstruction on both a grooved and a smooth plate. For the case of the riblets remarkable differences are observed:

- The average velocity profile near the wall is less steep.
- The areas of high speed fluid behind the obstruction and close to the wall are less intense.
- It seems that the wake behind the obstruction is longer.
- The trajectory of the head of the hairpin remains closer to the wall.

Briefly, an explanation will be given for the observations. A complication for the analysis is that in front of the obstruction also a standing (horseshoe) vortex is created with legs of opposite vorticity of those of the hairpin legs. These legs are conveyed at both sides of the hairpin. So in fact the complex combined structure of both horseshoe and hairpin has been studied. The results indicate that the interaction of horseshoe and hairpin leads to additional turbulent exchange phenomena and that this interaction is suppressed by the riblets. The interaction creates locally additional unstable conditions.

For a thorough study of purely the drag reducing abilities of riblets more experiments have to be carried out. The aim of the presentation is to discuss our experimental facilities, our tentative conclusions and the fact whether or not the artificial creation of coherent structures in combination with riblets is a useful method to understand drag reduction.



Figure 1: The upwelling of near-wall fluid at the edge of the wake area ($x/D \approx 1.5$) downstream of the hemisphere (side view, flow direction to the left).

DRAG REDUCTION USING GAS-BUBBLE SATURATION UNDER CONDITIONS OF THE LONGITUDINAL PRESSURE GRADIENT AND ELEVATED SURFACE ROUGHNESS

A.R. EVSEEV, L.I. MALTZEV, A.G. MALYUGA

Institute of Thermophysics, Siberian Branch of Russian Academy of Sciences. Novosibirsk,
630090, Russia

The report contains experimental results:

- distribution of skin friction along solid walls,
- profiles of mean velocity and gas fraction,
- pressure fluctuation data on a wall.

Experiments were carried out for near-wall liquid flow with gas microbubbles under conditions of the longitudinal pressure gradient and elevated surface roughness.